

Supplementary Material to: Bayesian Statistical Modeling of Spatially Correlated Error Structure in Atmospheric Tracer Inverse Analysis

C. Mukherjee, P. S. Kasibhatla, M. West

May 21, 2011

Abstract

This report details on the statistical aspects and presents all graphs and tables that are omitted in the main article.

1 Synthetic data simulation

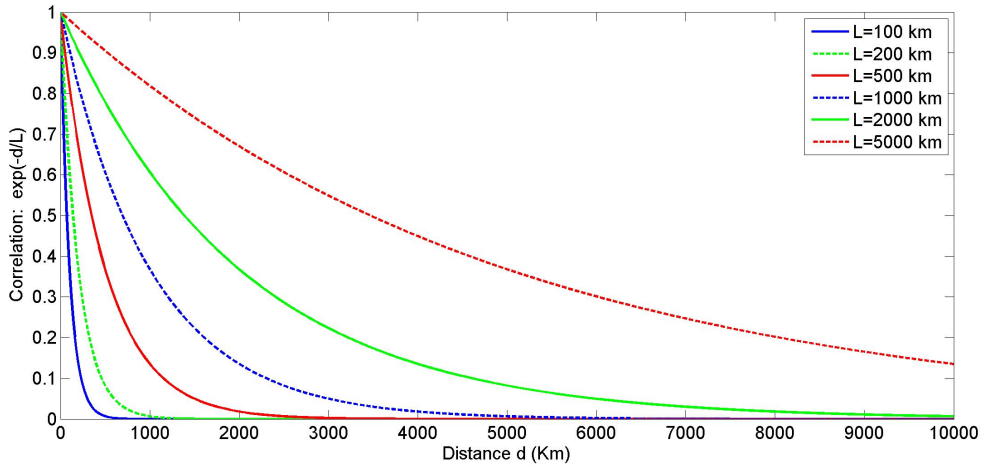


Figure 1: Exponential decay correlation kernel for different values of L .

2 Statistical Analysis

2.1 Prior specification

2.1.1 Prior on x

- Prior mean: $\mathbf{x}_a = (102.99, 95.2, 45.72, 108.72, 88.14, 41.03, 120.98, 21.99, 38.58, 88.28, 133.91, 146.51, 41.51, 28.05, 462.12)'$ in units of Tg CO year $^{-1}$.

- Prior standard deviations (specified to make coefficients of variation 0.5 for each source x_i .)
 $\{S_{a,i}^{1/2}\}_{i=1}^{15} = \{51.50, 47.60, 22.86, 54.36, 44.07, 20.52, 60.49, 11.00, 19.29, 44.14, 66.96, 73.26, 20.76, 14.03, 231.06\}$ in units of Tg CO year $^{-1}$.
- Truncated normal priors: $x_i \sim N(m_{a,i}, v_{a,i}) I(x_i > x_{a,i}/4)$.
- Moments of the truncated normal distribution $N(x | m, v) I(x > t)$: $\mathbb{E}(x) = m + v^{1/2} \lambda(\alpha)$, $\mathbb{V}(x) = v[1 - \delta(\alpha)]$ where $\alpha = (t - m)/v^{1/2}$, $\lambda(\alpha) = \phi(\alpha)/[1 - \Phi(\alpha)]$ and $\delta(\alpha) = \lambda(\alpha)[\lambda(\alpha) - \alpha]$.
- Solving for $x_{a,i} = m_{a,i} + v_{a,i}^{1/2} \lambda(\alpha)$ and $S_{a,i} = v_{a,i}[1 - \delta(\alpha)]$ where $\alpha = (x_{a,i}/4 - m_{a,i})/v_{a,i}^{1/2}$ we get:
 $\mathbf{m}_a = (72.92, 67.41, 32.37, 76.98, 62.41, 29.05, 85.66, 15.57, 27.32, 62.51, 94.82, 103.74, 29.39, 19.86, 327.21)'$ (in units of Tg CO year $^{-1}$) and
 $\mathbf{v}_a^{1/2} = (70.53, 65.19, 31.31, 74.45, 60.36, 28.10, 82.85, 15.06, 26.42, 60.45, 91.70, 100.33, 28.43, 19.21, 316.46)'$ (in units of Tg CO year $^{-1}$).

2.1.2 Prior on τ_n^2

$\tau_n^2 \sim IG(\alpha_n, \lambda_n)$ where the prior mean, $\mathbb{E}(\tau_n^2) = \lambda_n/(\alpha_n - 1) = \sigma^2$ (known, in units of 10^{18} molecules CO cm $^{-2}$) and prior variance, $\mathbb{V}(\tau_n^2) = \lambda_n^2/(\alpha_n - 1)^2(\alpha_n - 2) = 0.25 \times (\sigma^2)^2$ to make the coefficient of variation 0.5. Therefore $\alpha_n = 6$ and $\lambda_n = 5\sigma^2$.

2.1.3 Prior on τ_c^2

$\tau_c^2 \sim IG(\alpha_c, \lambda_c)$ where the prior mean, $\mathbb{E}(\tau_c^2) = \lambda_c/(\alpha_c - 1) = 8\sigma^2$, sets unbiased prior when there is no spatial dependence, i.e. $\rho = 0$. The prior variance, $\mathbb{V}(\tau_c^2) = \lambda_c^2/(\alpha_c - 1)^2(\alpha_c - 2) = 0.25 \times (8\sigma^2)^2 = 16\sigma^4$ to make the coefficient of variation 0.5. Therefore $\alpha_c = 6$ and $\lambda_c = 40\sigma^2$.

2.1.4 Prior on ρ

Uniform distribution $\rho : \rho \sim U(0, 1)$.

2.2 Markov Chain Monte Carlo for Posterior Computation

We present the posterior computation for the single time epoch case, generalization to the multiple time epoch is straightforward as discussed in the main article.

2.2.1 Complete Conditional distributions for the Non-spatial Model:

Updating x_i :

$$\begin{aligned}
\pi(x_i | m_{a,i}, v_{a,i}) &\propto N(x_i | m_{a,i}, v_{a,i}) I(x_i > x_{a,i}/4) \\
&\propto \exp\left\{-\frac{1}{2v_{a,i}}(x_i^2 - 2x_i m_{a,i})\right\} I(x_i > x_{a,i}/4) \\
L(\mathbf{y} | \mathbf{x}, \tau_n^2) &= N(\mathbf{y} | \mathbf{K}\mathbf{x}, \tau_n^2 \mathbf{I}) \propto \exp\left\{-\frac{1}{2\tau_n^2}(\mathbf{y} - \mathbf{K}\mathbf{x})'(\mathbf{y} - \mathbf{K}\mathbf{x})\right\} \\
&\propto \exp\left\{-\frac{1}{2\tau_n^2}(\mathbf{x}'\mathbf{K}'\mathbf{K}\mathbf{x} - 2\mathbf{x}'\mathbf{K}'\mathbf{y})\right\} \\
&\propto \exp\left(-\frac{1}{2\tau_n^2}[x_i^2(\mathbf{K}'_{(*,i)}\mathbf{K}_{(*,i)}) - 2x_i\{\mathbf{K}'_{(*,i)}(\mathbf{y} - \mathbf{K}_{(*,-i)}\mathbf{x}_{-i})\}]\right) \\
p(x_i | \mathbf{x}_{-i}, \mathbf{y}, \mathbf{m}_a, \mathbf{v}_a, \tau_n^2) &\propto \pi(x_i | m_{a,i}, v_{a,i}) \times L(\mathbf{y} | \mathbf{x}, \tau_n^2) \\
&\propto \exp\left(-\frac{1}{2}[x_i^2(1/v_{a,i} + 1/\tau_n^2 \mathbf{K}'_{(*,i)}\mathbf{K}_{(*,i)})\right. \\
&\quad \left.- 2x_i\{m_{a,i}/v_{a,i} + 1/\tau_n^2 \mathbf{K}'_{(*,i)}(\mathbf{y} - \mathbf{K}_{(*,-i)}\mathbf{x}_{-i})\}]) I(x_i > x_{a,i}/4) \\
&\propto N(x_i | E_{n,i}, V_{n,i}) I(x_i > x_{a,i}/4)
\end{aligned}$$

where $V_{n,i} = (1/v_{a,i} + 1/\tau_n^2 \mathbf{K}'_{(*,i)}\mathbf{K}_{(*,i)})^{-1}$ and $E_{n,i} = V_{n,i} \{m_{a,i}/v_{a,i} + 1/\tau_n^2 \mathbf{K}'_{(*,i)}(\mathbf{y} - \mathbf{K}_{(*,-i)}\mathbf{x}_{-i})\}$.

Updating τ_n^2 :

$$\begin{aligned}
\pi(\tau_n^2 | \alpha_n, \lambda_n) &= IG(\tau_n^2 | \alpha_n, \lambda_n) \propto (\tau_n^2)^{-(\alpha_n+1)} \exp\{-\lambda_n/\tau_n^2\} \\
L(\mathbf{y} | \mathbf{x}, \tau_n^2) &= N(\mathbf{y} | \mathbf{K}\mathbf{x}, \tau_n^2 \mathbf{I}) \\
&\propto |\tau_n^2 \mathbf{I}|^{-1/2} \exp\left\{-\frac{1}{2\tau_n^2}(\mathbf{y} - \mathbf{K}\mathbf{x})'(\mathbf{y} - \mathbf{K}\mathbf{x})\right\} \\
&\propto (\tau_n^2)^{-m/2} \exp\left\{-\frac{1}{2\tau_n^2}(\mathbf{y} - \mathbf{K}\mathbf{x})'(\mathbf{y} - \mathbf{K}\mathbf{x})\right\} \\
p(\tau_n^2 | \mathbf{y}, \mathbf{x}, \alpha_n, \lambda_n) &\propto \pi(\tau_n^2 | \alpha_n, \lambda_n) \times L(\mathbf{y} | \mathbf{x}, \tau_n^2) \\
&\propto (\tau_n^2)^{-(\alpha_n+m/2+1)} \exp\left[-\frac{1}{\tau_n^2}\{\lambda_n + \frac{1}{2}(\mathbf{y} - \mathbf{K}\mathbf{x})'(\mathbf{y} - \mathbf{K}\mathbf{x})\}\right] \\
&\propto IG[\tau_n^2 | \alpha_n + m/2, \lambda_n + \frac{1}{2}(\mathbf{y} - \mathbf{K}\mathbf{x})'(\mathbf{y} - \mathbf{K}\mathbf{x})]
\end{aligned}$$

Updating \mathbf{y}_M :

$$\begin{aligned}
p(\mathbf{y}_M | \mathbf{y}_H, \mathbf{x}, \tau_n^2) &\propto \pi(\mathbf{y}_M | \mathbf{x}, \tau_n^2) \times L(\mathbf{y}_H | \mathbf{y}_M, \mathbf{x}, \tau_n^2) \propto \pi(\mathbf{x}, \tau_n^2) \times L(\mathbf{y} | \mathbf{x}, \tau_n^2) \\
&\propto N(\mathbf{y} | \mathbf{K}\mathbf{x}, \tau_n^2 \mathbf{I}) \propto N[\mathbf{y}_M | \mathbf{K}_{(M,*)}\mathbf{x}, \tau_n^2 \mathbf{I}]
\end{aligned}$$

2.2.2 Complete Conditional distributions for the CAR model

Updating x_i : Remember that $\mathbf{U} = \tau_c^{-2} (\mathbf{D}_w - \rho \mathbf{W})$.

$$\begin{aligned}
\pi(x_i | m_{a,i}, v_{a,i}) &\propto N(x_i | m_{a,i}, v_{a,i}) I(x_i > x_{a,i}/4) \\
&\propto \exp\left\{-\frac{1}{2v_{a,i}}(x_i^2 - 2x_i m_{a,i})\right\} I(x_i > x_{a,i}/4) \\
L(\mathbf{y} | \mathbf{x}, \tau_c^2, \rho) &= N(\mathbf{y} | \mathbf{K}\mathbf{x}, \mathbf{U}^{-1}) \propto \exp\left\{-\frac{1}{2}(\mathbf{y} - \mathbf{K}\mathbf{x})' \mathbf{U}(\mathbf{y} - \mathbf{K}\mathbf{x})\right\} \\
&\propto \exp\left\{-\frac{1}{2}(\mathbf{x}' \mathbf{K}' \mathbf{U} \mathbf{K} \mathbf{x} - 2\mathbf{x}' \mathbf{K}' \mathbf{U} \mathbf{y})\right\} \\
&\propto \exp\left(-\frac{1}{2}[x_i^2 (\mathbf{K}'_{(*,i)} \mathbf{U} \mathbf{K}_{(*,i)}) - 2x_i \{\mathbf{K}_{(*,i)} \mathbf{U}(\mathbf{y} - \mathbf{K}_{(*,-i)} \mathbf{x}_{-i})\}]\right) \\
p(x_i | \mathbf{x}_{-i}, \mathbf{y}, \mathbf{m}_a, \mathbf{v}_a, \tau_c^2, \rho) &\propto \pi(x_i | m_{a,i}, v_{a,i}) \times L(\mathbf{y} | \mathbf{x}, \tau_c^2, \rho) \\
&\propto \exp\left(-\frac{1}{2}[x_i^2 (1/v_{a,i} + \mathbf{K}'_{(*,i)} \mathbf{U} \mathbf{K}_{(*,i)})\right. \\
&\quad \left.- 2x_i \{m_{a,i}/v_{a,i} + \mathbf{K}'_{(*,i)} \mathbf{U}(\mathbf{y} - \mathbf{K}_{(*,-i)} \mathbf{x}_{-i})\}]) I(x_i > x_{a,i}/4) \\
&\propto N(x_i | E_{c,i}, V_{c,i}) I(x_i > x_{a,i}/4)
\end{aligned}$$

where $V_{c,i} = (1/v_{a,i} + \mathbf{K}'_{(*,i)} \mathbf{U} \mathbf{K}_{(*,i)})^{-1}$ and $E_{c,i} = V_{c,i} \{m_{a,i}/v_{a,i} + \mathbf{K}'_{(*,i)} \mathbf{U}(\mathbf{y} - \mathbf{K}_{(*,-i)} \mathbf{x}_{-i})\}$.

Updating τ_c^2 :

$$\begin{aligned}
\pi(\tau_c^2 | \alpha_c, \lambda_c) &= IG(\tau_c^2 | \alpha_c, \lambda_c) \propto (\tau_c^2)^{-(\alpha_c+1)} \exp\{-\lambda_c/\tau_c^2\} \\
L(\mathbf{y} | \mathbf{x}, \tau_c^2, \rho) &= N[\mathbf{y} | \mathbf{K}\mathbf{x}, \tau_c^2 (\mathbf{D}_w - \rho \mathbf{W})^{-1}] \\
&\propto |\tau_c^2 (\mathbf{D}_w - \rho \mathbf{W})^{-1}|^{-1/2} \exp\left\{-\frac{1}{2\tau_c^2}(\mathbf{y} - \mathbf{K}\mathbf{x})' (\mathbf{D}_w - \rho \mathbf{W}) (\mathbf{y} - \mathbf{K}\mathbf{x})\right\} \\
&\propto (\tau_c^2)^{-m/2} \exp\left\{-\frac{1}{2\tau_c^2}(\mathbf{y} - \mathbf{K}\mathbf{x})' (\mathbf{D}_w - \rho \mathbf{W}) (\mathbf{y} - \mathbf{K}\mathbf{x})\right\} \\
p(\tau_c^2 | \mathbf{y}, \mathbf{x}, \alpha_c, \lambda_c, \rho) &\propto \pi(\tau_c^2 | \alpha_c, \lambda_c) \times L(\mathbf{y} | \mathbf{x}, \tau_c^2, \rho) \\
&\propto (\tau_c^2)^{-(\alpha_c+m/2+1)} \exp\left[-\frac{1}{\tau_c^2}\{\lambda_c + \frac{1}{2}(\mathbf{y} - \mathbf{K}\mathbf{x})' (\mathbf{D}_w - \rho \mathbf{W}) (\mathbf{y} - \mathbf{K}\mathbf{x})\}\right] \\
&\propto IG(\tau_c^2 | \alpha_c + m/2, \lambda_c + \frac{1}{2}(\mathbf{y} - \mathbf{K}\mathbf{x})' (\mathbf{D}_w - \rho \mathbf{W}) (\mathbf{y} - \mathbf{K}\mathbf{x}))
\end{aligned}$$

Updating ρ :

$$\begin{aligned}
\pi(\rho) &= \text{Unif}(0, 1) \propto I(0 < \rho < 1) \\
L(\mathbf{y} | \mathbf{x}, \tau_c^2, \rho) &= N[\mathbf{y} | \mathbf{K}\mathbf{x}, \tau_c^2 (\mathbf{D}_w - \rho \mathbf{W})^{-1}] \\
p(\rho | \mathbf{y}, \mathbf{x}, \alpha_c, \lambda_c, \tau_c^2) &\propto \pi(\rho) \times L(\mathbf{y} | \mathbf{x}, \tau_c^2, \rho) \\
&\propto N[\mathbf{y} | \mathbf{K}\mathbf{x}, \tau_c^2 (\mathbf{D}_w - \rho \mathbf{W})^{-1}] I(0 < \rho < 1)
\end{aligned}$$

We update ρ with a random-walk Metropolis step. It involves sampling $\rho^* \sim N(\rho^* | \rho, s^2) I(0 < \rho < 1)$ and accepting it with probability

$$\alpha = \min\left\{1, \frac{p(\rho^* | \mathbf{y}, \mathbf{x}, \alpha_c, \lambda_c, \tau_c^2)}{p(\rho | \mathbf{y}, \mathbf{x}, \alpha_c, \lambda_c, \tau_c^2)}\right\} = \min\left\{1, \frac{N[\mathbf{y} | \mathbf{K}\mathbf{x}, \tau_c^2 (\mathbf{D}_w - \rho^* \mathbf{W})^{-1}]}{N[\mathbf{y} | \mathbf{K}\mathbf{x}, \tau_c^2 (\mathbf{D}_w - \rho \mathbf{W})^{-1}]}\right\}$$

If accepted we set $\rho = \rho^*$. The step size s is determined adaptively during the burn-in.

Updating \mathbf{y}_M :

$$\begin{aligned} p(\mathbf{y}_M \mid \mathbf{y}_H, \mathbf{x}, \tau_c^2, \rho) &\propto \pi(\mathbf{y}_M \mid \mathbf{x}, \tau_c^2, \rho) \times L(\mathbf{y}_H \mid \mathbf{y}_M, \mathbf{x}, \tau_c^2, \rho) \propto \pi(\mathbf{x}, \tau_c^2, \rho) \times L(\mathbf{y} \mid \mathbf{x}, \mathbf{U}^{-1}) \\ &\propto N(\mathbf{y} \mid \mathbf{K}\mathbf{x}, \mathbf{U}^{-1}) \propto N[\mathbf{y}_M \mid \mathbf{K}_{(M,*)}\mathbf{x} - \mathbf{U}_{M,M}^{-1}\mathbf{U}_{M,H}(\mathbf{y}_H - \mathbf{K}_{(H,*)}\mathbf{x}), \mathbf{U}_{M,M}^{-1}] \end{aligned}$$

2.3 Results:

Tables 1 - 6 presents the posterior summary for the CO fluxes and model parameters for the synthetic data analysis. We point out that τ_c^2 itself is not the marginal variance for the CAR model as τ_n^2 is for the NS model. This is because $\tau_c^2(D_w - \rho W)^{-1}$ is the model covariance matrix and $(D_w - \rho W)^{-1}$ has non-unity diagonal elements. The diagonal elements of this matrix are not identical for a finite lattice due to edge effects — we can use the posterior distribution of i^{th} diagonal element of \mathbf{U}^{-1} for an interior lattice point i as the marginal variance. Table 7 presents the summary statistics for the grid box with center at latitude = $-2^\circ N$ and longitude = $7.5^\circ E$. These values are to be compared with $\sigma^2 = 0.1240$ that was used to simulate the synthetic data.

Figures 2 - 7 plots the posterior predictive samples from non-spatial model and the CAR model for different values of L . Figures 8 - 22 shows the scatter plots of “true” x_i versus estimated x_i for each source category for different values of L .

Table 1: Summary of posterior inferences for the CO fluxes (in units of Tg CO year $^{-1}$) and model parameters from analysis of synthetic data with $L = 100$ km.

	Truth		Prior		NS Model		NS Model		CAR model		CAR model	
		mean	(SD)	mean	(SD)	95% CI	mean	(SD)	mean	(SD)	95% CI	
x_1	68.68	102.99	(51.49)	63.81	(7.17)	[49.65, 77.73]	63.52	(7.65)	[48.59, 78.36]			
x_2	91.73	95.20	(47.60)	77.43	(11.02)	[55.71, 99.09]	73.33	(12.07)	[49.11, 97.01]			
x_3	29.63	45.72	(22.86)	56.73	(11.29)	[33.98, 78.52]	59.73	(12.06)	[36.06, 83.49]			
x_4	109.93	108.72	(54.36)	108.33	(7.35)	[94.21, 122.62]	108.89	(7.60)	[94.09, 123.73]			
x_5	28.86	88.14	(44.07)	25.37	(6.57)	[12.50, 38.23]	24.72	(6.89)	[11.20, 38.31]			
x_6	24.70	41.03	(20.51)	23.33	(5.75)	[12.02, 34.54]	23.19	(5.96)	[11.67, 34.81]			
x_7	141.32	120.98	(60.49)	151.08	(11.52)	[128.41, 173.67]	153.54	(12.13)	[129.81, 177.83]			
x_8	19.96	21.99	(10.99)	17.56	(3.22)	[11.19, 23.85]	17.64	(3.33)	[10.95, 24.29]			
x_9	55.40	38.58	(19.29)	55.77	(3.46)	[48.89, 62.54]	55.62	(3.65)	[48.34, 62.81]			
x_{10}	56.15	88.28	(44.14)	63.25	(3.15)	[57.06, 69.35]	63.14	(3.30)	[56.69, 69.53]			
x_{11}	155.44	133.91	(66.95)	158.80	(3.84)	[151.47, 166.33]	158.74	(4.06)	[150.79, 166.68]			
x_{12}	263.06	146.51	(73.25)	263.40	(3.18)	[257.27, 269.62]	263.10	(3.27)	[256.72, 269.52]			
x_{13}	11.81	41.51	(20.75)	11.99	(4.29)	[3.65, 20.26]	12.30	(4.53)	[3.45, 21.07]			
x_{14}	54.93	28.05	(14.02)	53.77	(3.83)	[46.32, 61.36]	54.44	(4.15)	[46.43, 62.58]			
x_{15}	382.36	462.12	(231.06)	363.74	(15.51)	[333.33, 394.11]	362.83	(16.67)	[330.44, 395.19]			
τ_n^2	0.1240	0.0620		0.1244	(1.4e-3)							
τ_c^2	0.9920	(0.4960)					0.0074	(8.2e-5)	[0.0073, 0.0076]			
ρ	0.5000	(0.2890)					0.02921	(1.7e-2)	[0.00180, 0.06696]			

Table 2: Summary of posterior inferences for the CO fluxes (in units of Tg CO year⁻¹) and model parameters from analysis of synthetic data with L = 200 km.

	Truth	Prior mean	Prior (SD)	NS Model mean	NS Model (SD)	NS Model 95% CI	CAR model mean	CAR model (SD)	CAR model 95% CI
x_1	68.68	102.99	(51.49)	76.74	(7.10)	[63.13, 90.61]	77.02	(9.08)	[59.06, 94.62]
x_2	91.73	95.20	(47.60)	87.59	(10.97)	[66.21, 109.15]	90.68	(13.71)	[63.82, 117.89]
x_3	29.63	45.72	(22.86)	40.94	(11.22)	[19.14, 62.97]	39.59	(13.38)	[13.11, 65.96]
x_4	109.93	108.72	(54.36)	107.51	(7.33)	[93.13, 121.94]	108.19	(8.92)	[90.70, 125.54]
x_5	28.86	88.14	(44.07)	21.47	(6.52)	[8.55, 34.26]	20.60	(7.93)	[5.08, 36.42]
x_6	24.70	41.03	(20.51)	27.74	(5.67)	[16.40, 38.74]	27.60	(6.90)	[14.17, 41.14]
x_7	141.32	120.98	(60.49)	125.85	(11.44)	[103.14, 148.09]	126.56	(13.95)	[99.44, 154.10]
x_8	19.96	21.99	(10.99)	21.22	(3.16)	[14.98, 27.40]	20.69	(3.93)	[13.04, 28.48]
x_9	55.40	38.58	(19.29)	49.27	(3.46)	[42.62, 56.14]	48.76	(4.26)	[40.59, 57.17]
x_{10}	56.15	88.28	(44.14)	59.63	(3.13)	[53.43, 65.77]	59.77	(3.82)	[52.47, 67.28]
x_{11}	155.44	133.91	(66.95)	150.88	(3.80)	[143.36, 158.28]	150.11	(4.71)	[140.86, 159.28]
x_{12}	263.06	146.51	(73.25)	261.42	(3.15)	[255.30, 267.65]	260.55	(3.89)	[252.81, 268.22]
x_{13}	11.81	41.51	(20.75)	14.49	(4.30)	[6.04, 22.85]	14.49	(5.21)	[4.26, 24.87]
x_{14}	54.93	28.05	(14.02)	54.07	(3.81)	[46.64, 61.44]	52.78	(4.60)	[43.88, 61.90]
x_{15}	382.36	462.12	(231.06)	391.45	(15.46)	[361.58, 421.92]	393.32	(18.83)	[356.41, 430.24]
τ_n^2	0.1240	(0.0620)		0.1234	(1.3e-3)				
τ_c^2	0.9920	(0.4960)					0.0071	(8.0e-5)	[0.0070, 0.0073]
ρ	0.5000	(0.2890)					0.36092	(2.0e-2)	[0.32240, 0.40007]

Table 3: Summary of posterior inferences for the CO fluxes (in units of Tg CO year⁻¹) and model parameters from analysis of synthetic data with L = 500 km.

	Truth	Prior mean	Prior (SD)	NS Model mean	NS Model (SD)	NS Model 95% CI	CAR model mean	CAR model (SD)	CAR model 95% CI
x_1	68.68	102.99	(51.49)	72.00	(7.29)	[57.62, 86.09]	88.81	(15.72)	[57.84, 119.50]
x_2	91.73	95.20	(47.60)	71.33	(11.12)	[49.28, 92.95]	64.45	(19.63)	[25.41, 102.92]
x_3	29.63	45.72	(22.86)	63.59	(11.47)	[41.44, 86.39]	59.57	(16.92)	[26.31, 93.07]
x_4	109.93	108.72	(54.36)	108.51	(7.49)	[93.88, 123.11]	108.22	(14.70)	[79.17, 137.03]
x_5	28.86	88.14	(44.07)	22.24	(6.70)	[9.17, 35.34]	24.32	(12.66)	[-0.19, 49.10]
x_6	24.70	41.03	(20.51)	40.69	(5.84)	[29.42, 52.13]	40.56	(10.47)	[20.35, 61.31]
x_7	141.32	120.98	(60.49)	133.02	(11.74)	[110.38, 156.06]	142.38	(22.03)	[99.54, 185.47]
x_8	19.96	21.99	(10.99)	20.44	(3.25)	[13.99, 26.83]	23.06	(6.09)	[11.23, 35.02]
x_9	55.40	38.58	(19.29)	52.39	(3.49)	[45.54, 59.29]	46.75	(6.88)	[33.05, 60.14]
x_{10}	56.15	88.28	(44.14)	63.90	(3.19)	[57.70, 70.16]	61.80	(6.72)	[48.72, 74.86]
x_{11}	155.44	133.91	(66.95)	150.48	(3.96)	[142.88, 158.23]	152.24	(7.97)	[136.50, 167.64]
x_{12}	263.06	146.51	(73.25)	263.62	(3.23)	[257.25, 270.06]	264.95	(6.55)	[252.14, 277.49]
x_{13}	11.81	41.51	(20.75)	15.19	(4.45)	[6.39, 23.79]	13.41	(7.97)	[-2.37, 28.62]
x_{14}	54.93	28.05	(14.02)	56.83	(3.83)	[49.42, 64.35]	56.77	(6.02)	[44.90, 68.72]
x_{15}	382.36	462.12	(231.06)	358.25	(15.75)	[327.74, 389.17]	343.56	(31.06)	[282.81, 404.22]
τ_n^2	0.1240	(0.0620)		0.1297	(1.4e-3)				
τ_c^2	0.9920	(0.4960)					0.0051	(5.9e-5)	[0.0050, 0.0052]
ρ	0.5000	(0.2890)					0.91812	(6.2e-3)	[0.90534, 0.93000]

Table 4: Summary of posterior inferences for the CO fluxes (in units of Tg CO year⁻¹) and model parameters from analysis of synthetic data with L = 1000 km.

	Truth	Prior mean	Prior (SD)	NS Model mean	NS Model (SD)	NS Model 95% CI	CAR model mean	CAR model (SD)	CAR model 95% CI
x_1	68.68	102.99	(51.49)	71.01	(7.17)	[56.78, 85.10]	78.19	(18.19)	[42.52, 113.47]
x_2	91.73	95.20	(47.60)	27.47	(10.88)	[6.24, 48.44]	102.78	(20.37)	[61.92, 141.94]
x_3	29.63	45.72	(22.86)	74.26	(11.17)	[52.74, 95.94]	29.11	(17.18)	[-4.23, 63.05]
x_4	109.93	108.72	(54.36)	89.87	(7.40)	[75.38, 104.48]	82.99	(15.56)	[52.04, 113.19]
x_5	28.86	88.14	(44.07)	37.36	(6.60)	[24.52, 50.38]	42.51	(13.38)	[15.94, 68.70]
x_6	24.70	41.03	(20.51)	-16.73	(5.73)	[-28.06, -5.52]	23.75	(11.25)	[1.80, 45.68]
x_7	141.32	120.98	(60.49)	142.31	(11.45)	[119.90, 164.86]	133.72	(23.41)	[87.70, 178.61]
x_8	19.96	21.99	(10.99)	31.85	(3.21)	[25.62, 38.26]	24.06	(6.70)	[10.88, 37.20]
x_9	55.40	38.58	(19.29)	51.34	(3.49)	[44.59, 58.01]	49.18	(7.42)	[34.44, 63.80]
x_{10}	56.15	88.28	(44.14)	37.51	(3.09)	[31.49, 43.52]	53.32	(7.51)	[38.74, 67.92]
x_{11}	155.44	133.91	(66.95)	163.29	(3.88)	[155.56, 170.96]	160.96	(8.52)	[144.35, 177.67]
x_{12}	263.06	146.51	(73.25)	248.06	(3.21)	[241.74, 254.42]	260.62	(6.97)	[246.85, 274.20]
x_{13}	11.81	41.51	(20.75)	53.29	(4.37)	[44.75, 61.66]	23.17	(8.25)	[6.99, 39.33]
x_{14}	54.93	28.05	(14.02)	50.99	(3.79)	[43.51, 58.27]	53.09	(5.52)	[42.08, 63.85]
x_{15}	382.36	462.12	(231.06)	444.51	(15.46)	[413.98, 474.73]	399.44	(35.54)	[329.20, 469.50]
τ_n^2	0.1240	(0.0620)		0.1237	(1.4e-3)				
τ_c^2	0.9920	(0.4960)					0.0032	(3.6e-5)	[0.0031, 0.0033]
ρ	0.5000	(0.2890)					0.99141	(1.7e-3)	[0.98803, 0.99461]

Table 5: Summary of posterior inferences for the CO fluxes (in units of Tg CO year⁻¹) and model parameters from analysis of synthetic data with L = 2000 km.

	Truth	Prior mean	Prior (SD)	NS Model mean	NS Model (SD)	NS Model 95% CI	CAR model mean	CAR model (SD)	CAR model 95% CI
x_1	68.68	102.99	(51.49)	53.74	(6.94)	[40.04, 67.51]	61.43	(16.26)	[29.94, 93.28]
x_2	91.73	95.20	(47.60)	115.87	(10.66)	[94.96, 136.88]	101.15	(18.23)	[65.07, 137.11]
x_3	29.63	45.72	(22.86)	55.32	(10.99)	[33.62, 76.61]	32.81	(15.76)	[2.06, 63.50]
x_4	109.93	108.72	(54.36)	98.01	(7.09)	[83.99, 111.91]	100.39	(13.13)	[74.64, 126.34]
x_5	28.86	88.14	(44.07)	72.27	(6.36)	[59.60, 84.49]	48.05	(11.42)	[25.58, 70.55]
x_6	24.70	41.03	(20.51)	20.17	(5.52)	[9.29, 30.82]	18.88	(10.31)	[-1.73, 38.75]
x_7	141.32	120.98	(60.49)	173.51	(11.02)	[151.61, 194.83]	151.08	(21.09)	[109.90, 192.47]
x_8	19.96	21.99	(10.99)	41.25	(3.10)	[35.19, 47.38]	22.26	(6.01)	[10.44, 33.85]
x_9	55.40	38.58	(19.29)	42.37	(3.35)	[35.77, 48.91]	57.69	(6.51)	[45.13, 70.50]
x_{10}	56.15	88.28	(44.14)	72.55	(3.06)	[66.52, 78.62]	59.21	(6.39)	[46.51, 71.71]
x_{11}	155.44	133.91	(66.95)	176.55	(3.74)	[169.15, 183.90]	169.03	(7.08)	[155.32, 182.98]
x_{12}	263.06	146.51	(73.25)	259.51	(3.07)	[253.46, 265.57]	267.86	(5.86)	[256.36, 279.11]
x_{13}	11.81	41.51	(20.75)	7.70	(4.17)	[-0.48, 15.83]	13.76	(7.14)	[-0.39, 27.68]
x_{14}	54.93	28.05	(14.02)	60.20	(3.66)	[53.10, 67.29]	48.60	(4.66)	[39.54, 57.68]
x_{15}	382.36	462.12	(231.06)	281.78	(14.83)	[252.96, 310.69]	359.77	(32.35)	[296.90, 423.20]
τ_n^2	0.1240	(0.0620)		0.1159	(1.3e-3)				
τ_c^2	0.9920	(0.4960)					0.0020	(2.3e-5)	[0.0020, 0.0021]
ρ	0.5000	(0.2890)					0.99882	(4.1e-4)	[0.99790, 0.99952]

Table 6: Summary of posterior inferences for the CO fluxes (in units of Tg CO year⁻¹) and model parameters from analysis of synthetic data with L = 5000 km.

	Truth	Prior mean	Prior (SD)	NS Model mean	NS Model (SD)	NS Model 95% CI	CAR model mean	CAR model (SD)	CAR model 95% CI
x_1	68.68	102.99	(51.49)	93.25	(6.58)	[80.25, 106.28]	68.18	(12.87)	[42.43, 93.38]
x_2	91.73	95.20	(47.60)	81.82	(10.24)	[61.42, 101.98]	98.82	(14.85)	[70.42, 128.08]
x_3	29.63	45.72	(22.86)	-19.91	(10.50)	[-40.84, 0.79]	6.49	(13.74)	[-20.67, 33.60]
x_4	109.93	108.72	(54.36)	155.01	(6.71)	[141.85, 168.12]	119.93	(10.44)	[99.41, 140.44]
x_5	28.86	88.14	(44.07)	-29.04	(5.98)	[-40.80, -17.33]	22.86	(9.13)	[4.65, 41.07]
x_6	24.70	41.03	(20.51)	24.96	(5.29)	[14.64, 35.40]	21.51	(8.44)	[4.74, 38.09]
x_7	141.32	120.98	(60.49)	202.24	(10.46)	[182.04, 222.59]	152.97	(16.81)	[120.20, 186.08]
x_8	19.96	21.99	(10.99)	2.56	(2.94)	[-3.24, 8.28]	7.80	(4.95)	[-1.84, 17.43]
x_9	55.40	38.58	(19.29)	18.04	(3.15)	[11.86, 24.35]	52.72	(5.19)	[42.47, 62.98]
x_{10}	56.15	88.28	(44.14)	53.08	(2.84)	[47.50, 58.61]	54.31	(4.95)	[44.58, 64.33]
x_{11}	155.44	133.91	(66.95)	198.83	(3.49)	[192.00, 205.62]	157.03	(5.52)	[146.39, 167.93]
x_{12}	263.06	146.51	(73.25)	244.24	(2.89)	[238.50, 249.92]	263.03	(4.52)	[254.28, 272.09]
x_{13}	11.81	41.51	(20.75)	21.24	(3.93)	[13.59, 28.99]	9.90	(5.71)	[-1.29, 20.97]
x_{14}	54.93	28.05	(14.02)	82.51	(3.49)	[75.83, 89.40]	56.71	(3.74)	[49.44, 63.92]
x_{15}	382.36	462.12	(231.06)	343.71	(14.31)	[315.91, 371.63]	356.87	(25.81)	[306.36, 408.22]
τ_n^2	0.1240	(0.0620)		0.1026	(1.1e-3)				
τ_c^2	0.9920	(0.4960)					0.0012	(1.4e-5)	[0.0012, 0.0012]
ρ	0.5000	(0.2890)					0.99969	(1.3e-4)	[0.99940, 0.99989]

Table 7: Estimated CAR marginal variance for the synthetic data analysis.

L (in km)	mean (SD) (in 10 ¹⁸ molecules CO cm ⁻²)	95% CI (in 10 ¹⁸ molecules CO cm ⁻²)
100	0.1208 (0.0013)	[0.1182, 0.1234]
200	0.1199 (0.0013)	[0.1173, 0.1245]
500	0.1232 (0.0023)	[0.1189, 0.1277]
1000	0.1142 (0.0084)	[0.1027, 0.1347]
2000	0.1101 (0.0250)	[0.0812, 0.1751]
5000	0.1018 (0.0379)	[0.0581, 0.2018]

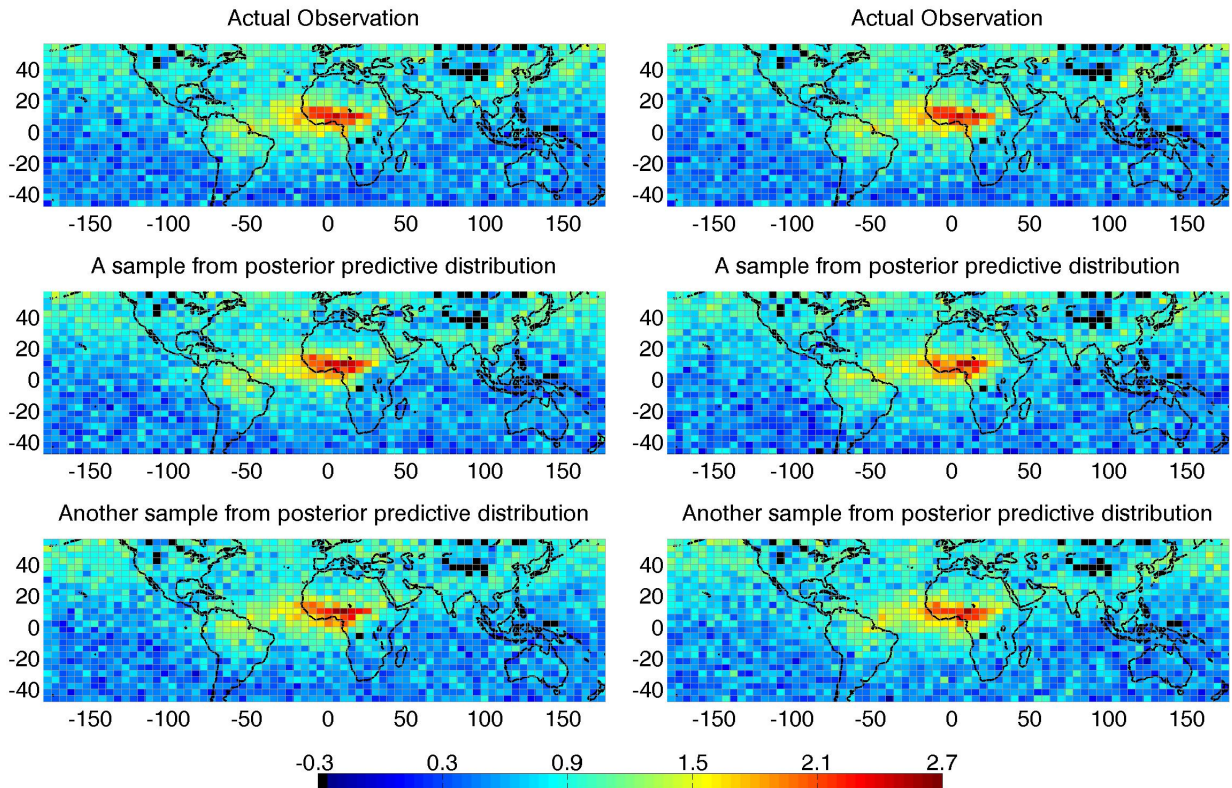


Figure 2: Two samples of column CO fields (in units of 10^{18} molecules CO cm^{-2}) from the posterior predictive distributions of NS (lower 2 left panels) and CAR (lower 2 right panels) models for December 2000 for $L = 100 \text{ km}$; top panels show the corresponding synthetic data.

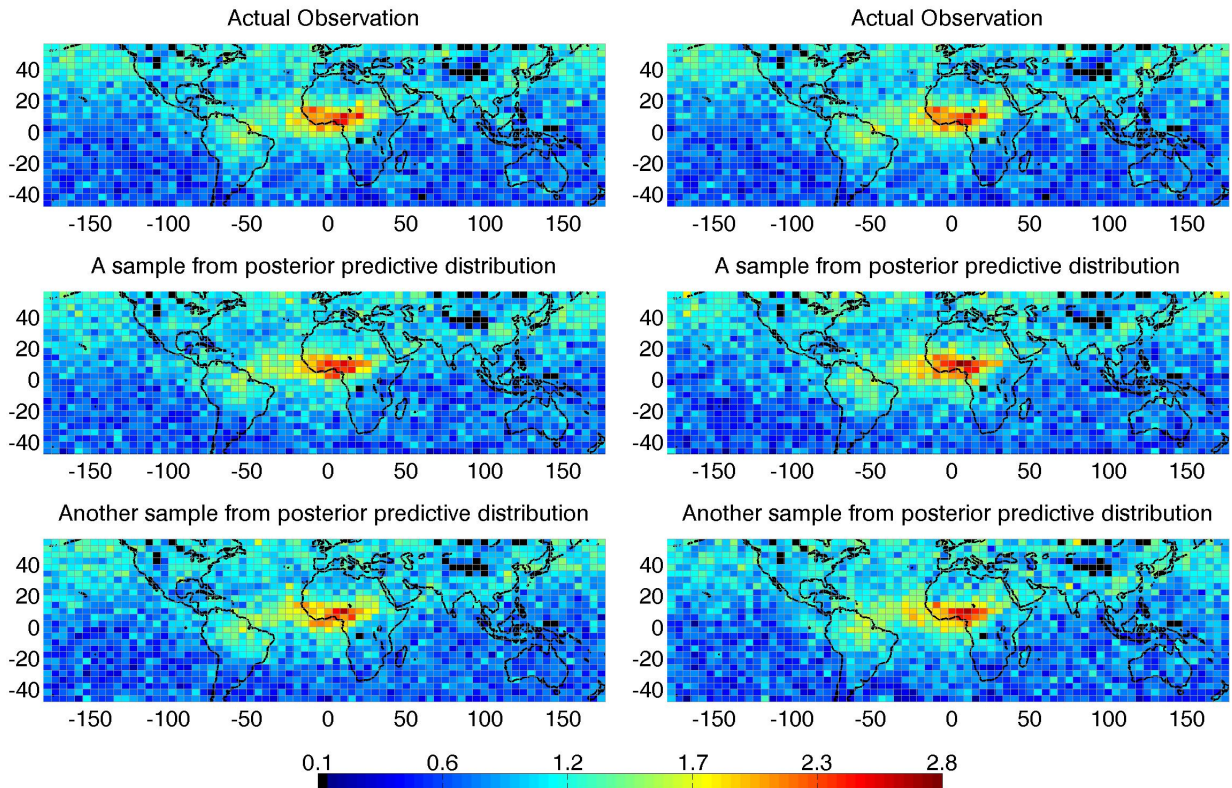


Figure 3: Two samples of column CO fields (in units of 10^{18} molecules CO cm^{-2}) from the posterior predictive distributions of NS (lower 2 left panels) and CAR (lower 2 right panels) models for December 2000 for $L = 200 \text{ km}$; top panels show the corresponding synthetic data.

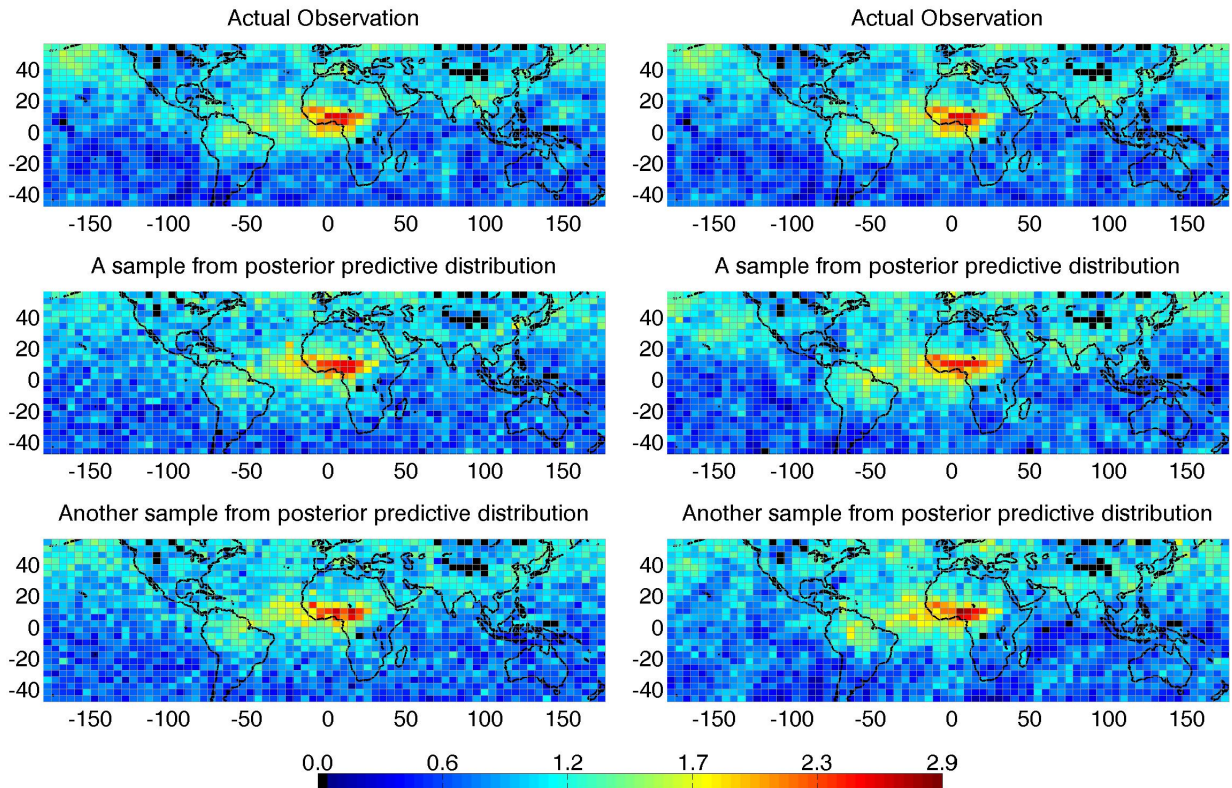


Figure 4: Two samples of column CO fields (in units of 10^{18} molecules CO cm^{-2}) from the posterior predictive distributions of NS (lower 2 left panels) and CAR (lower 2 right panels) models for December 2000 for $L = 500$ km; top panels show the corresponding synthetic data.

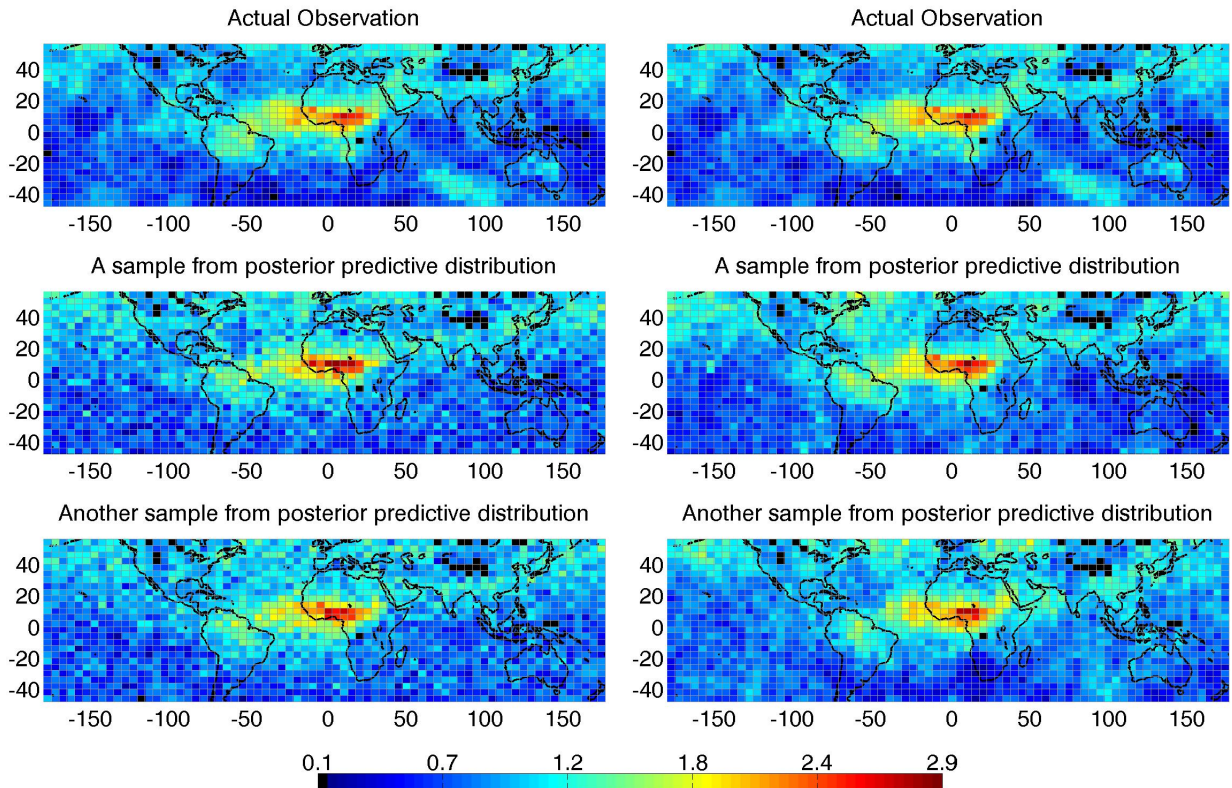


Figure 5: Two samples of column CO fields (in units of 10^{18} molecules CO cm^{-2}) from the posterior predictive distributions of NS (lower 2 left panels) and CAR (lower 2 right panels) models for December 2000 for $L = 1000$ km; top panels show the corresponding synthetic data.

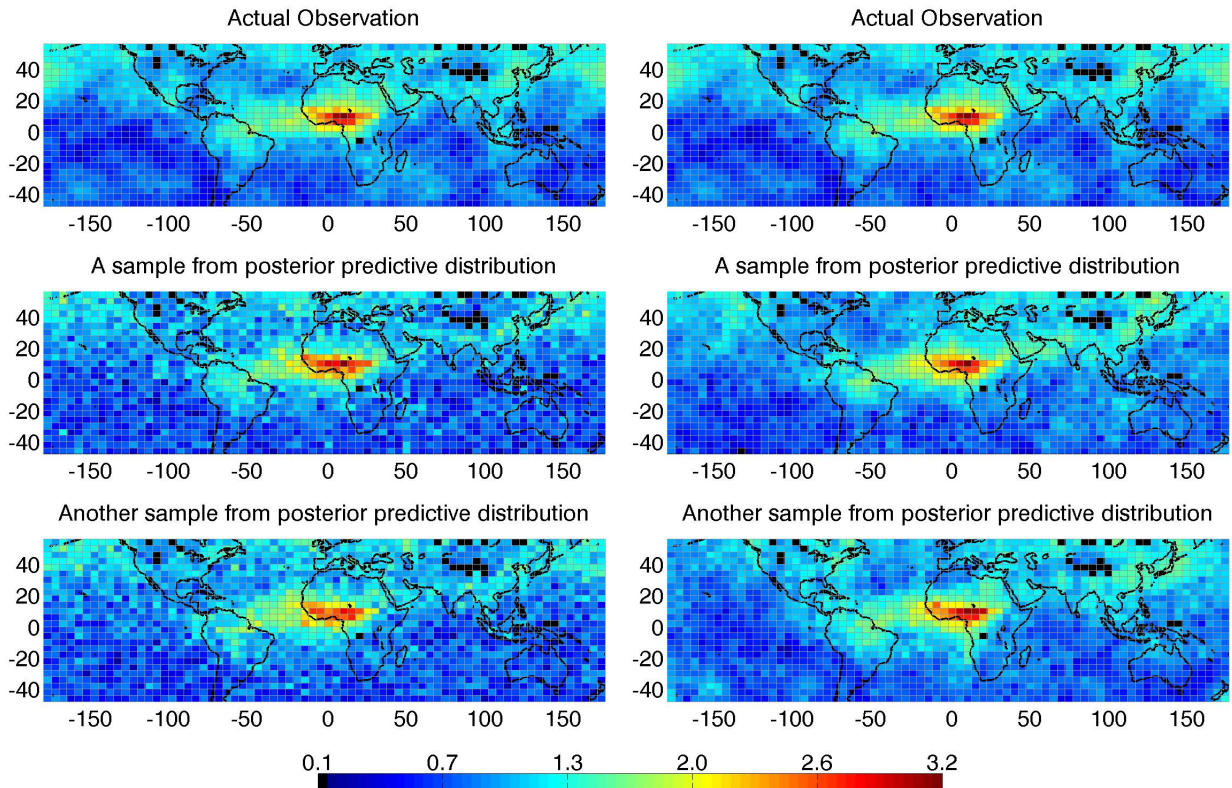


Figure 6: Two samples of column CO fields (in units of 10^{18} molecules CO cm^{-2}) from the posterior predictive distributions of NS (lower 2 left panels) and CAR (lower 2 right panels) models for December 2000 for $L = 2000$ km; top panels show the corresponding synthetic data.

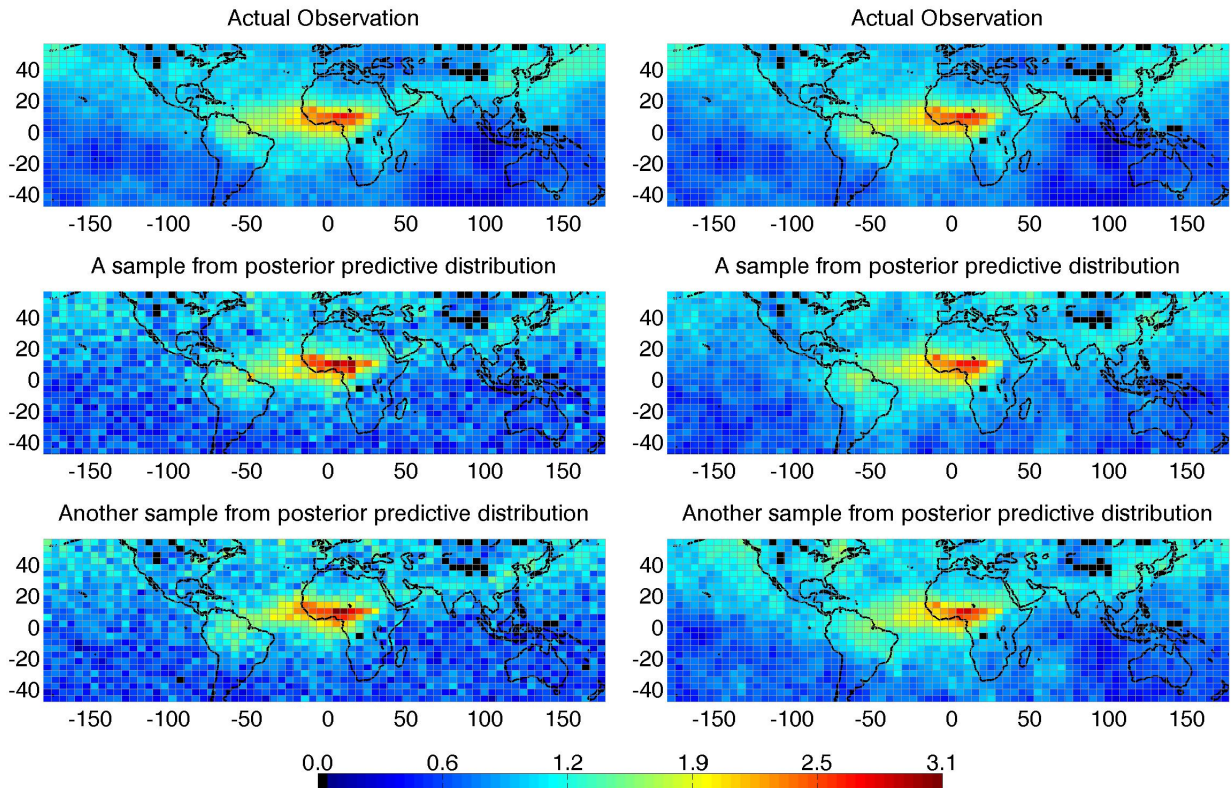


Figure 7: Two samples of column CO fields (in units of 10^{18} molecules CO cm^{-2}) from the posterior predictive distributions of NS (lower 2 left panels) and CAR (lower 2 right panels) models for December 2000 for $L = 5000$ km; top panels show the corresponding synthetic data.

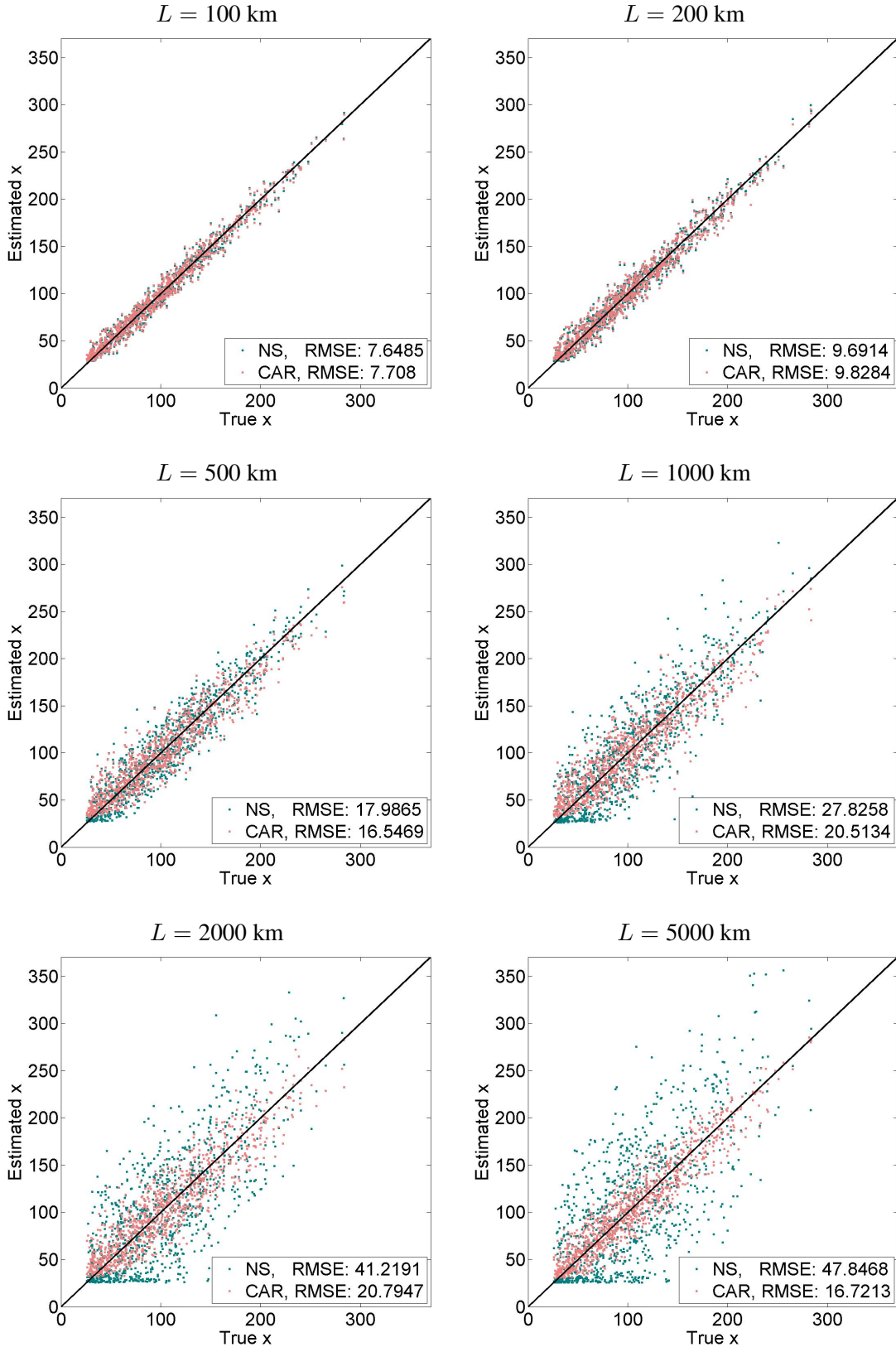


Figure 8: Scatter plots of “true” x_i versus estimated x_i (in units of Tg CO year $^{-1}$) for the source category FFBF-NAM computed from 1,000 synthetic data sets.

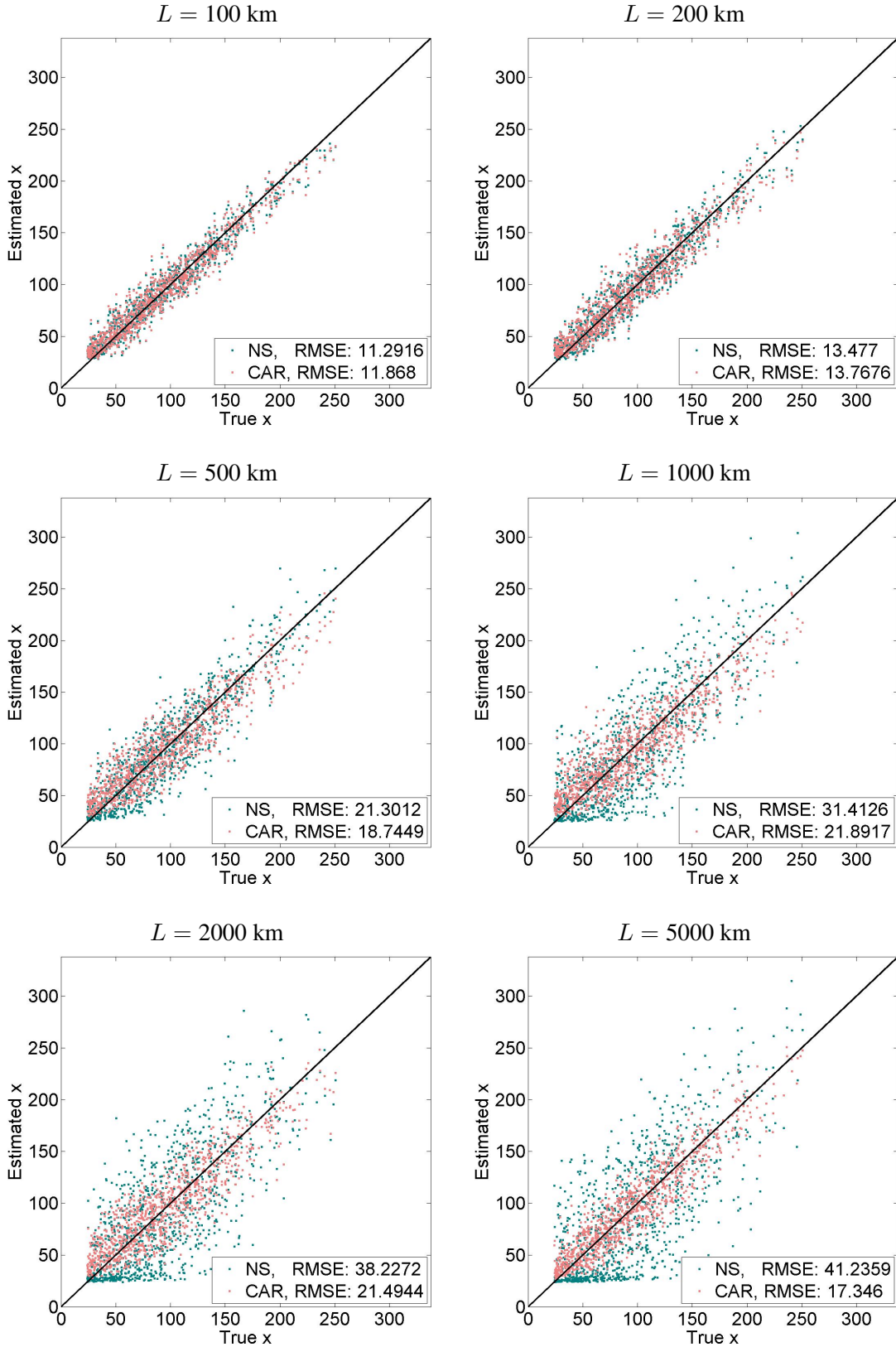


Figure 9: Scatter plots of “true” x_i versus estimated x_i (in units of Tg CO year $^{-1}$) for the source category FFBF-EUR computed from 1,000 synthetic data sets.

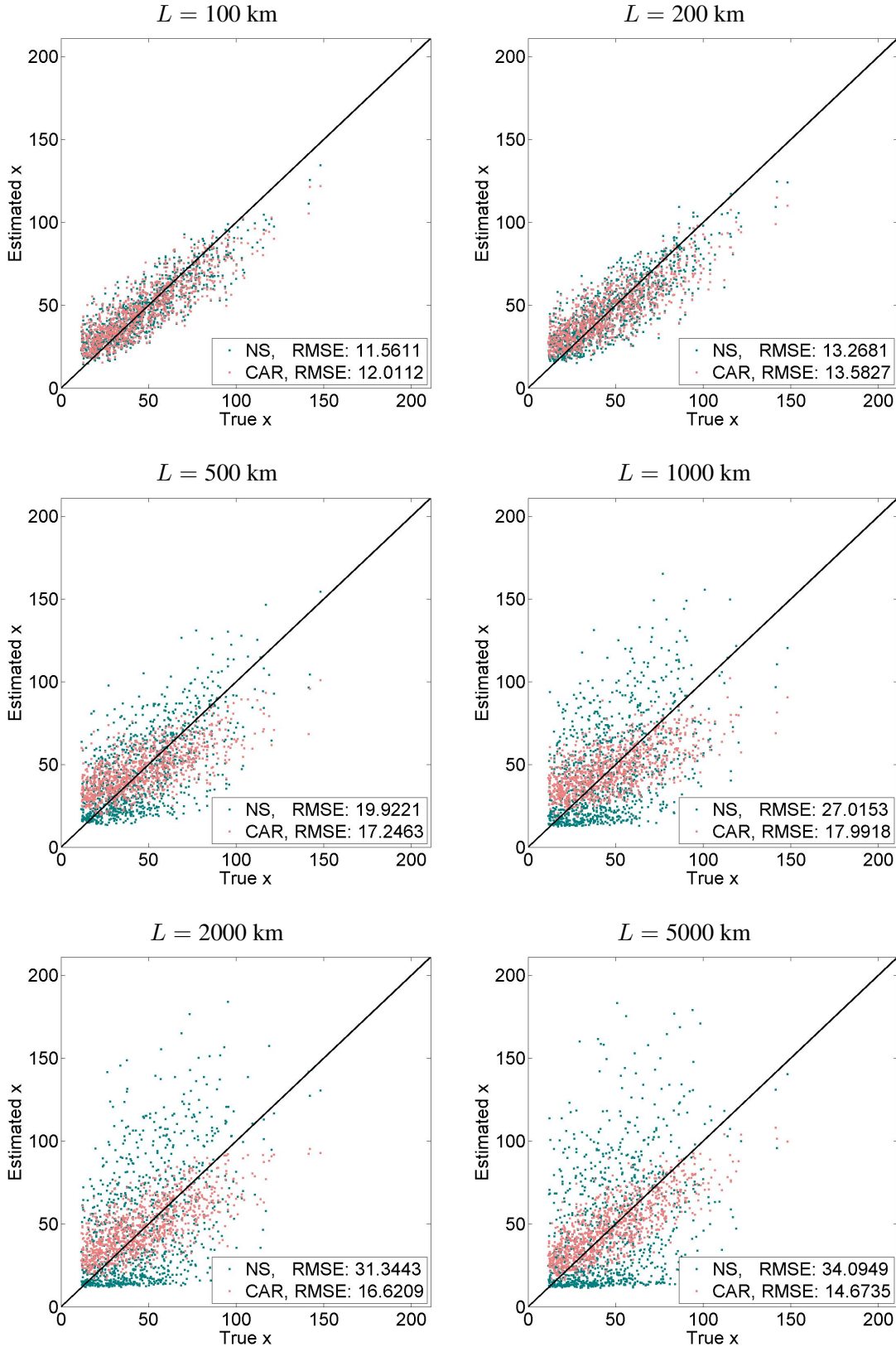


Figure 10: Scatter plots of “true” x_i versus estimated x_i (in units of Tg CO year $^{-1}$) for the source category FFBF-RUS computed from 1,000 synthetic data sets.

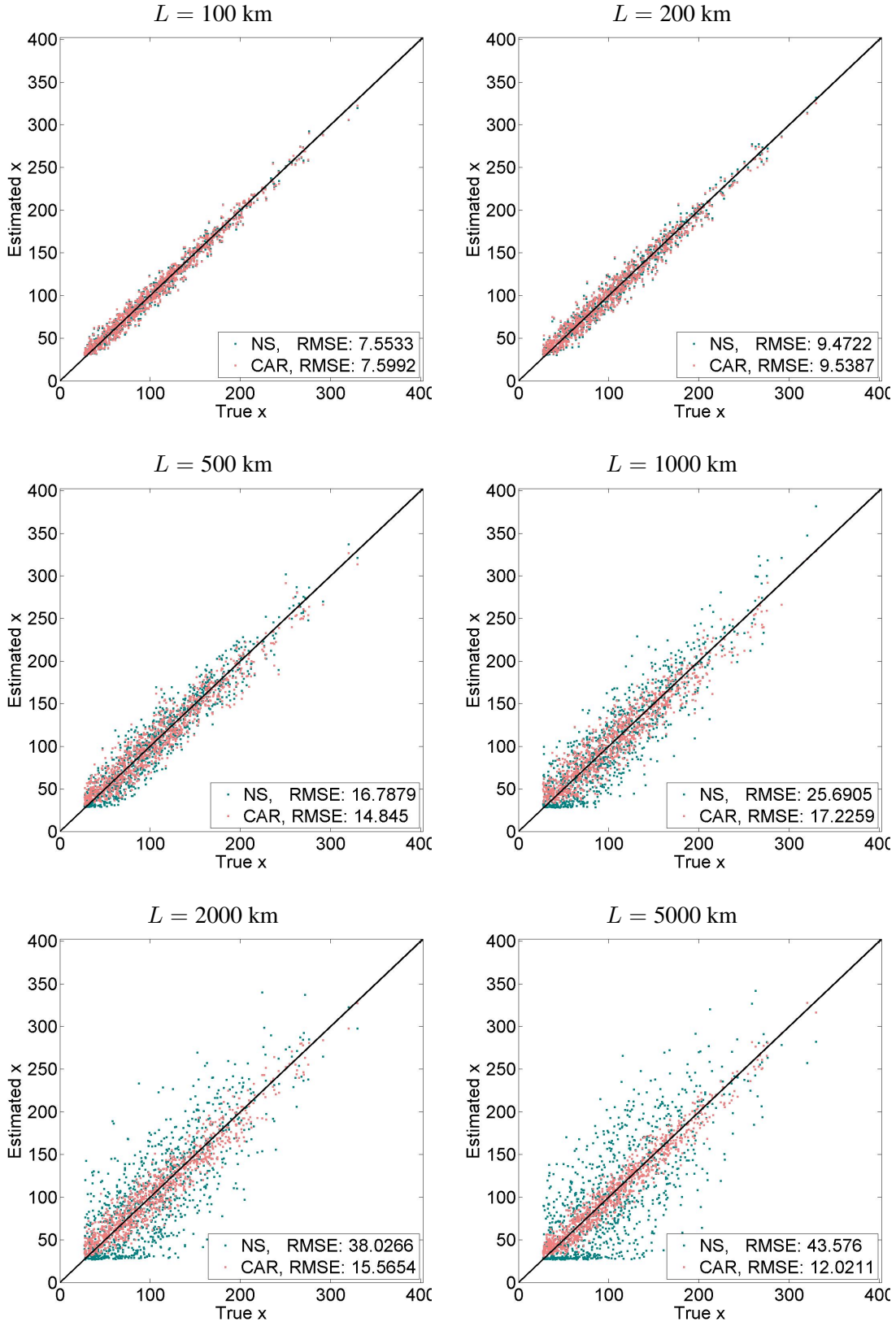


Figure 11: Scatter plots of “true” x_i versus estimated x_i (in units of Tg CO year $^{-1}$) for the source category FFBF-EAS computed from 1,000 synthetic data sets.

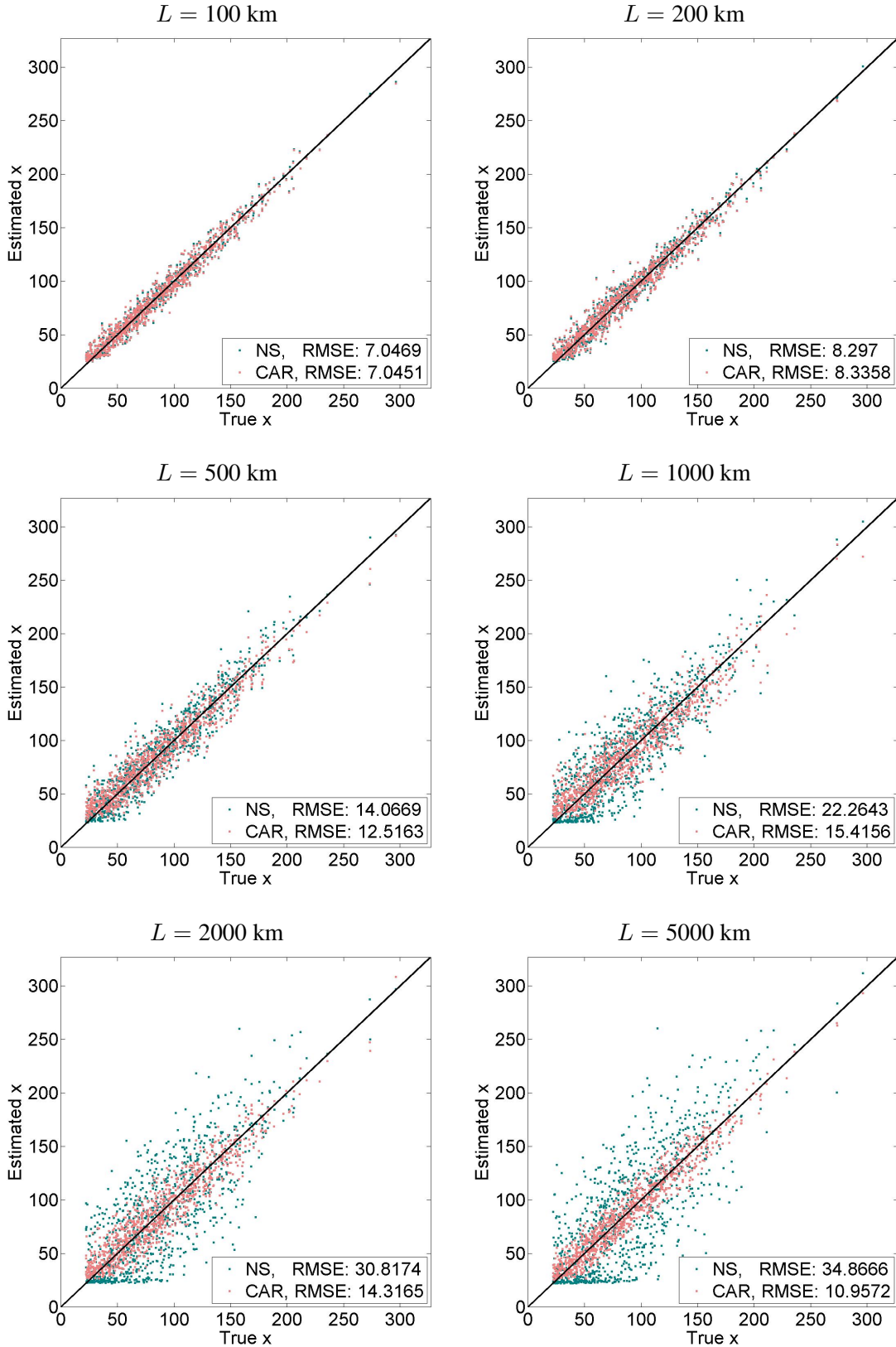


Figure 12: Scatter plots of “true” x_i versus estimated x_i (in units of Tg CO year $^{-1}$) for the source category FFBF-SAS computed from 1,000 synthetic data sets.

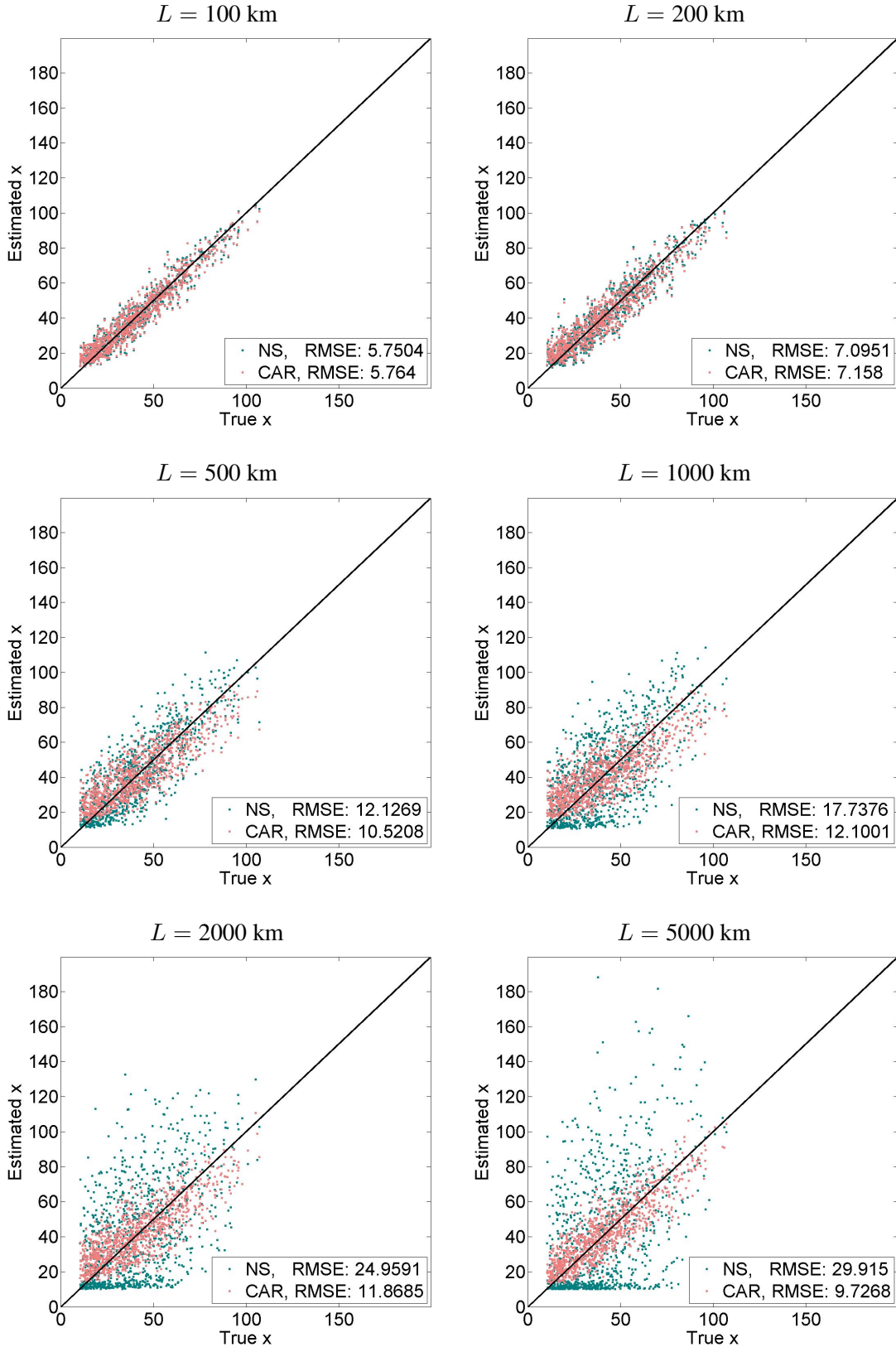


Figure 13: Scatter plots of “true” x_i versus estimated x_i (in units of Tg CO year $^{-1}$) for the source category FFBF-SEA computed from 1,000 synthetic data sets.

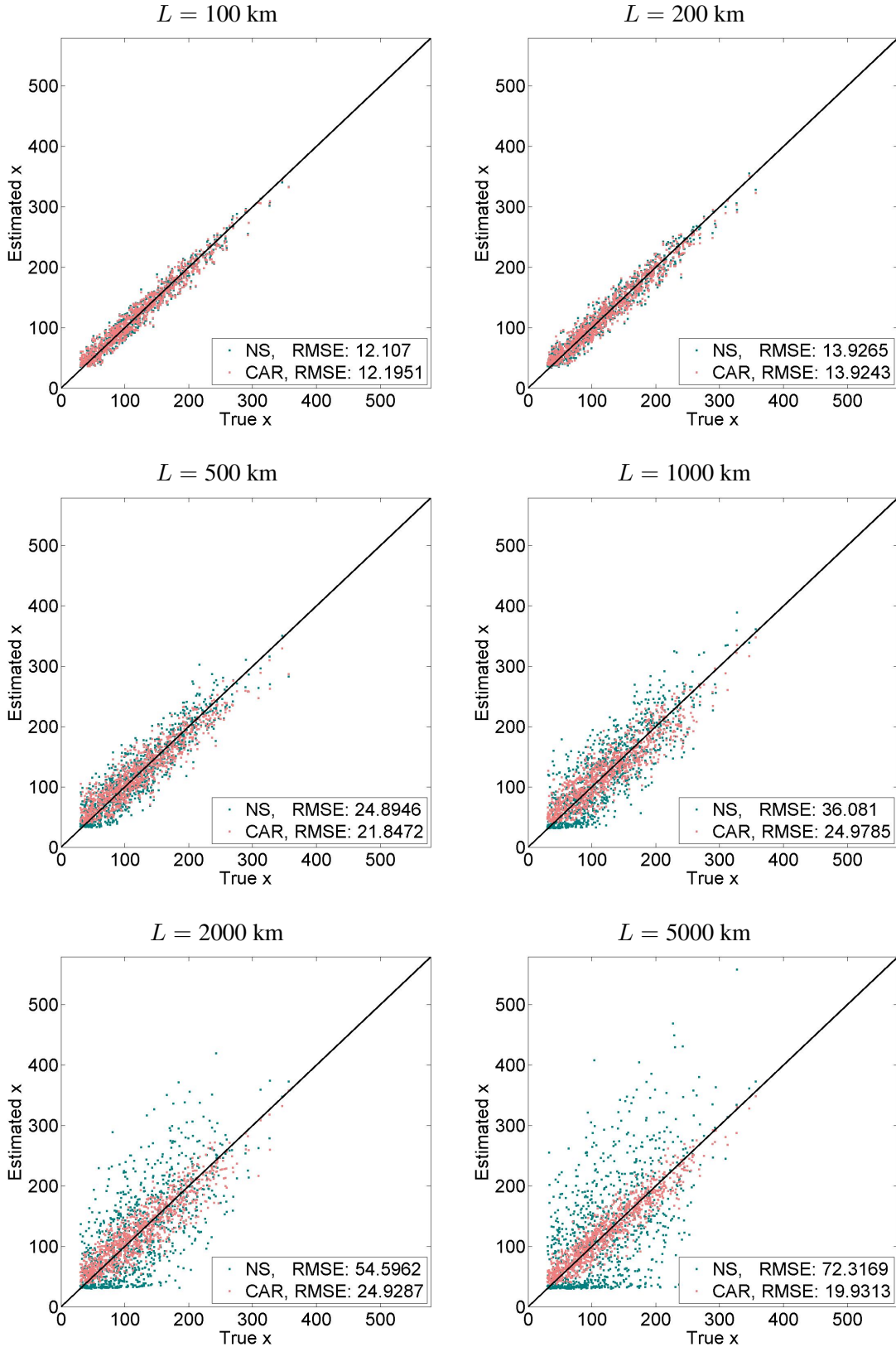


Figure 14: Scatter plots of “true” x_i versus estimated x_i (in units of Tg CO year $^{-1}$) for the source category FFBF-ROW computed from 1,000 synthetic data sets.

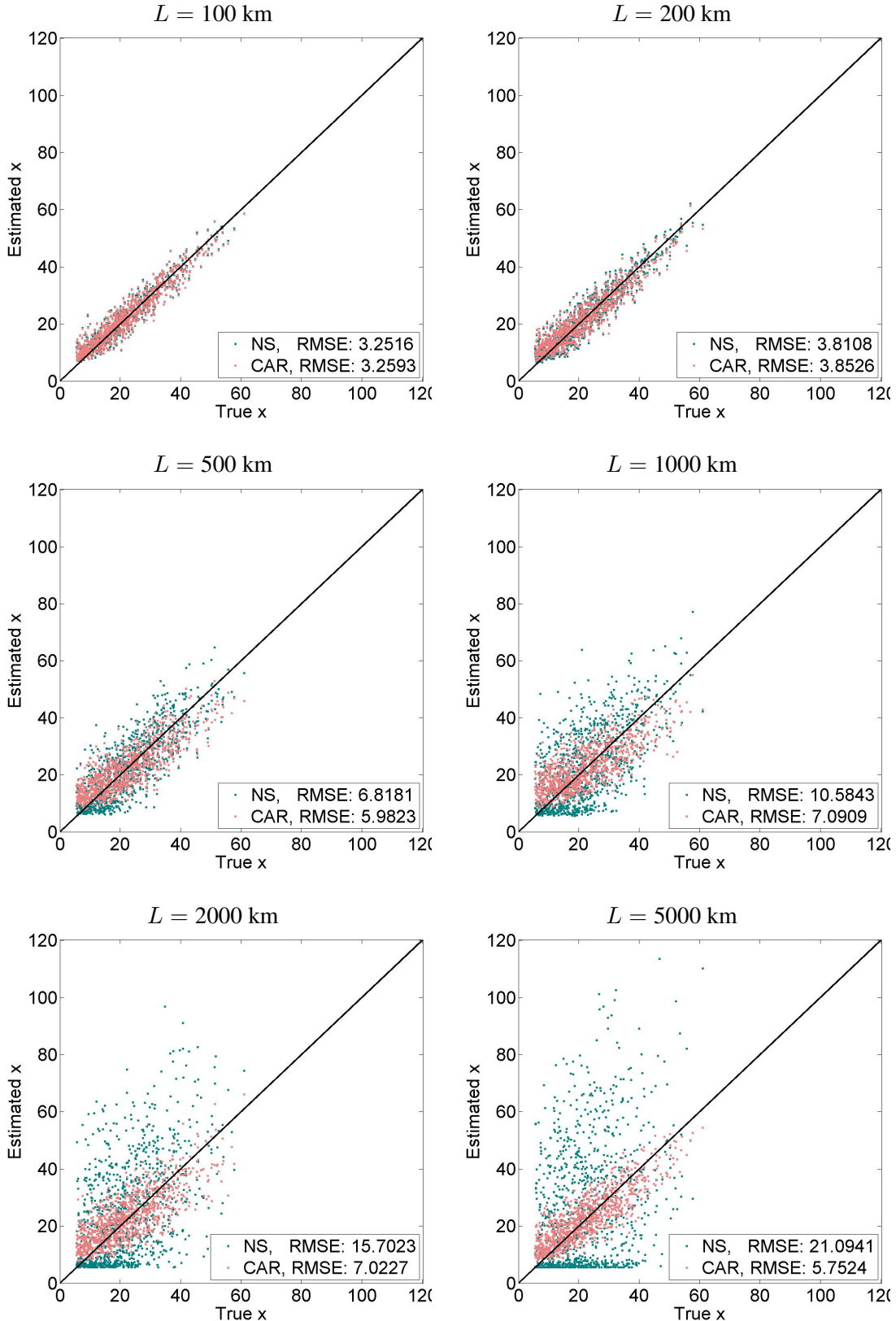


Figure 15: Scatter plots of “true” x_i versus estimated x_i (in units of Tg CO year $^{-1}$) for the source category BIOM-OTH computed from 1,000 synthetic data sets.

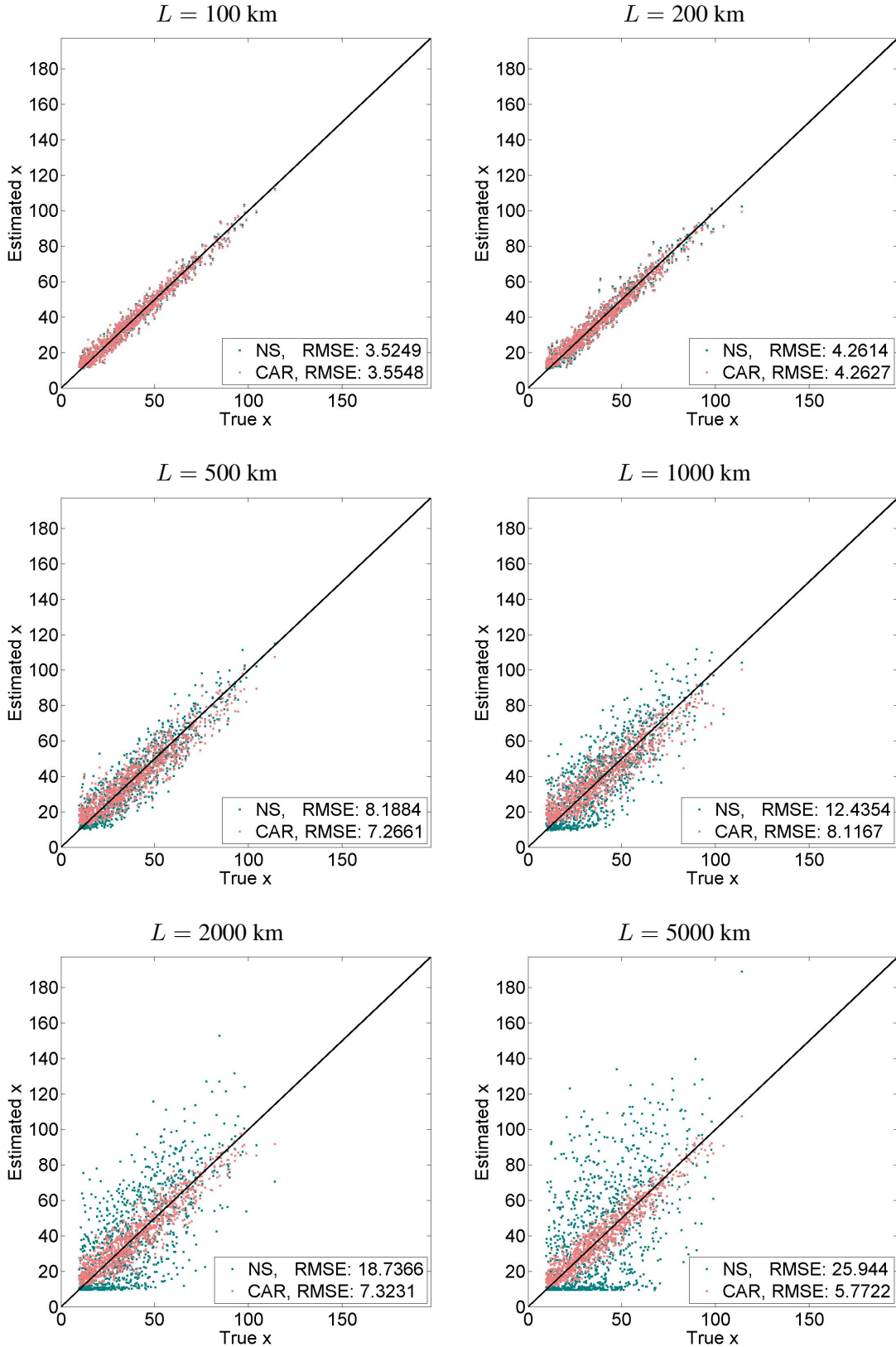


Figure 16: Scatter plots of “true” x_i versus estimated x_i (in units of Tg CO year $^{-1}$) for the source category BIOM-NLA computed from 1,000 synthetic data sets.

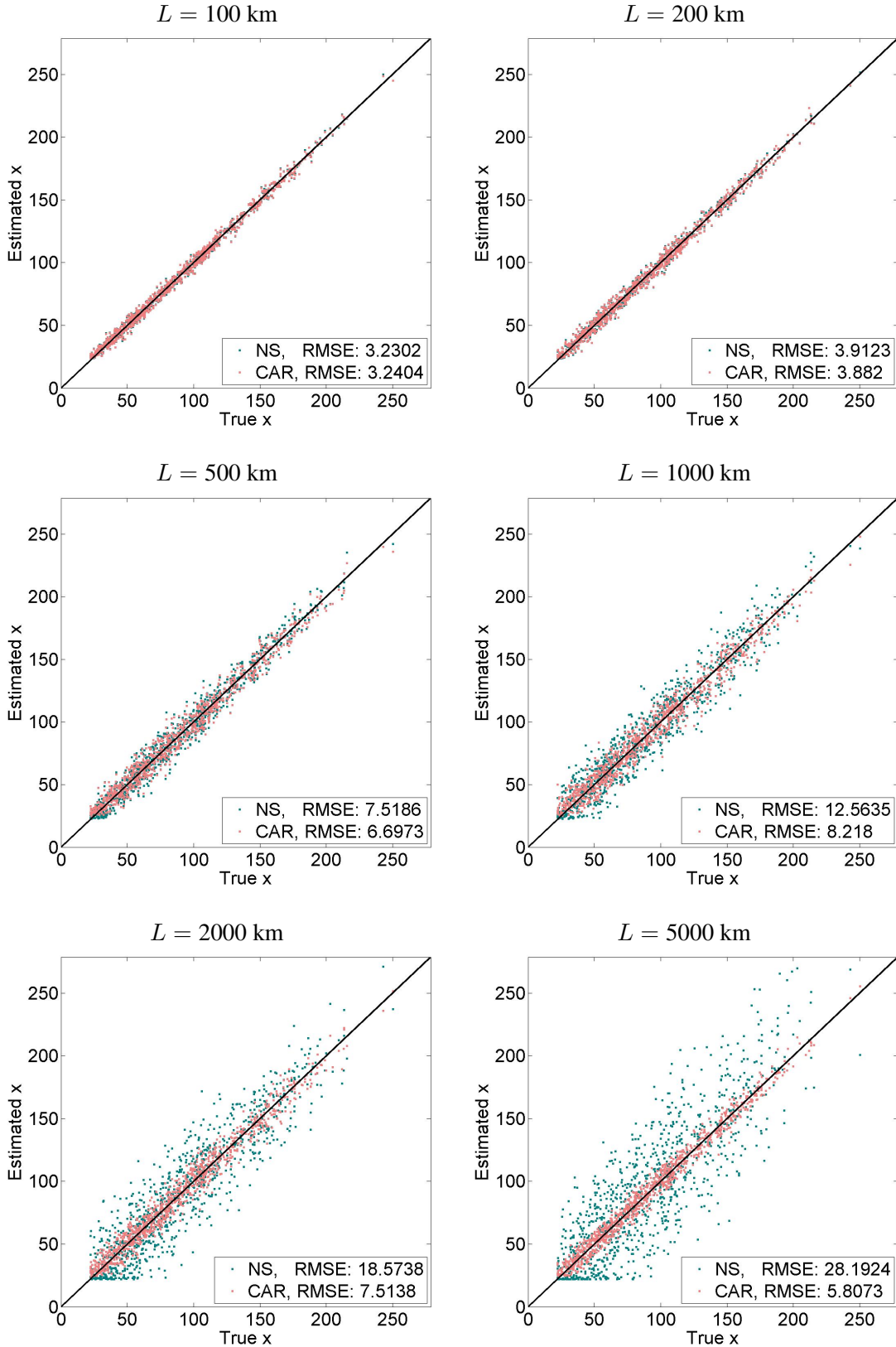


Figure 17: Scatter plots of “true” x_i versus estimated x_i (in units of Tg CO year $^{-1}$) for the source category BIOM-SLA computed from 1,000 synthetic data sets.

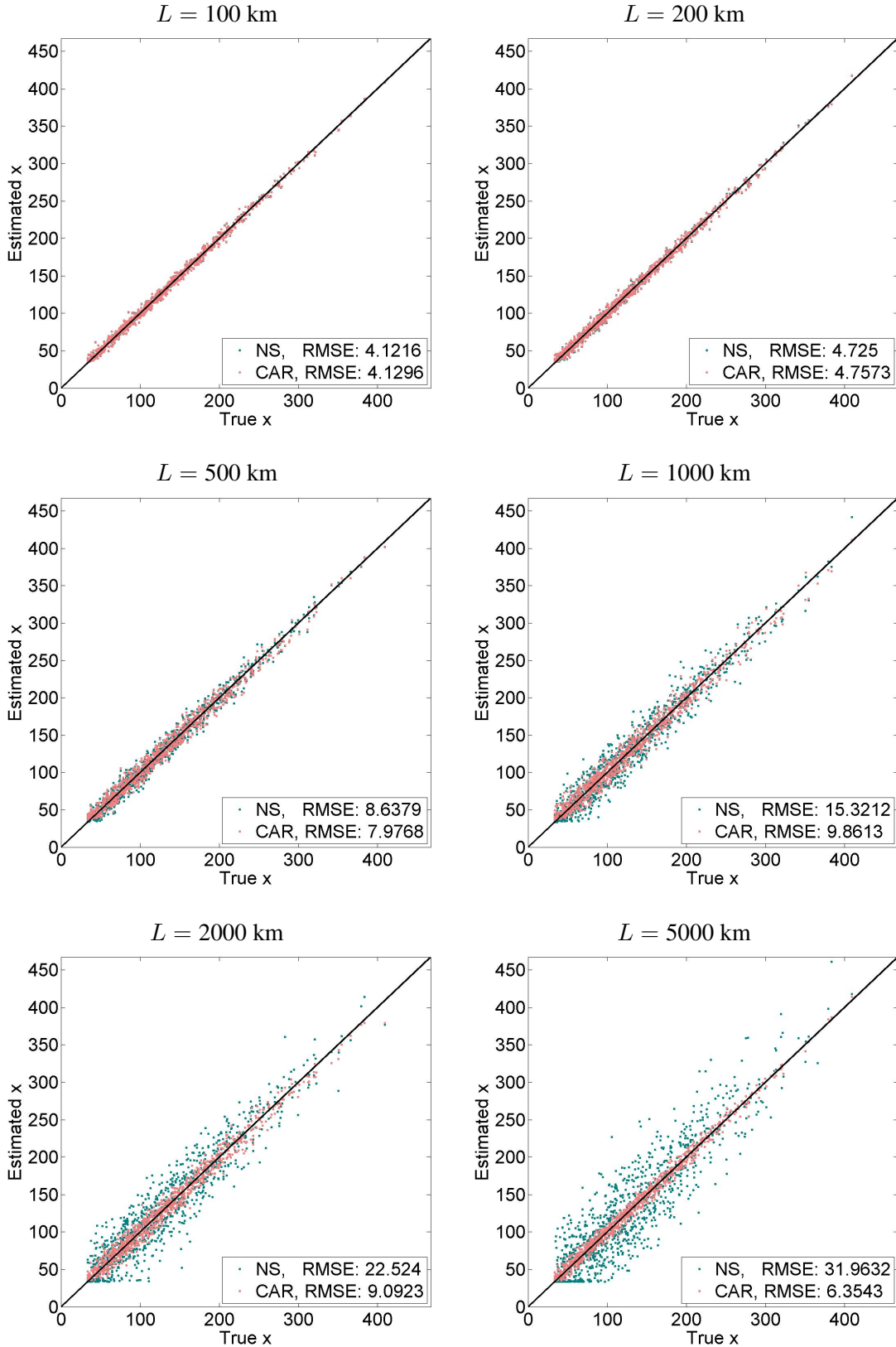


Figure 18: Scatter plots of “true” x_i versus estimated x_i (in units of Tg CO year $^{-1}$) for the source category BIOM-NAF computed from 1,000 synthetic data sets.

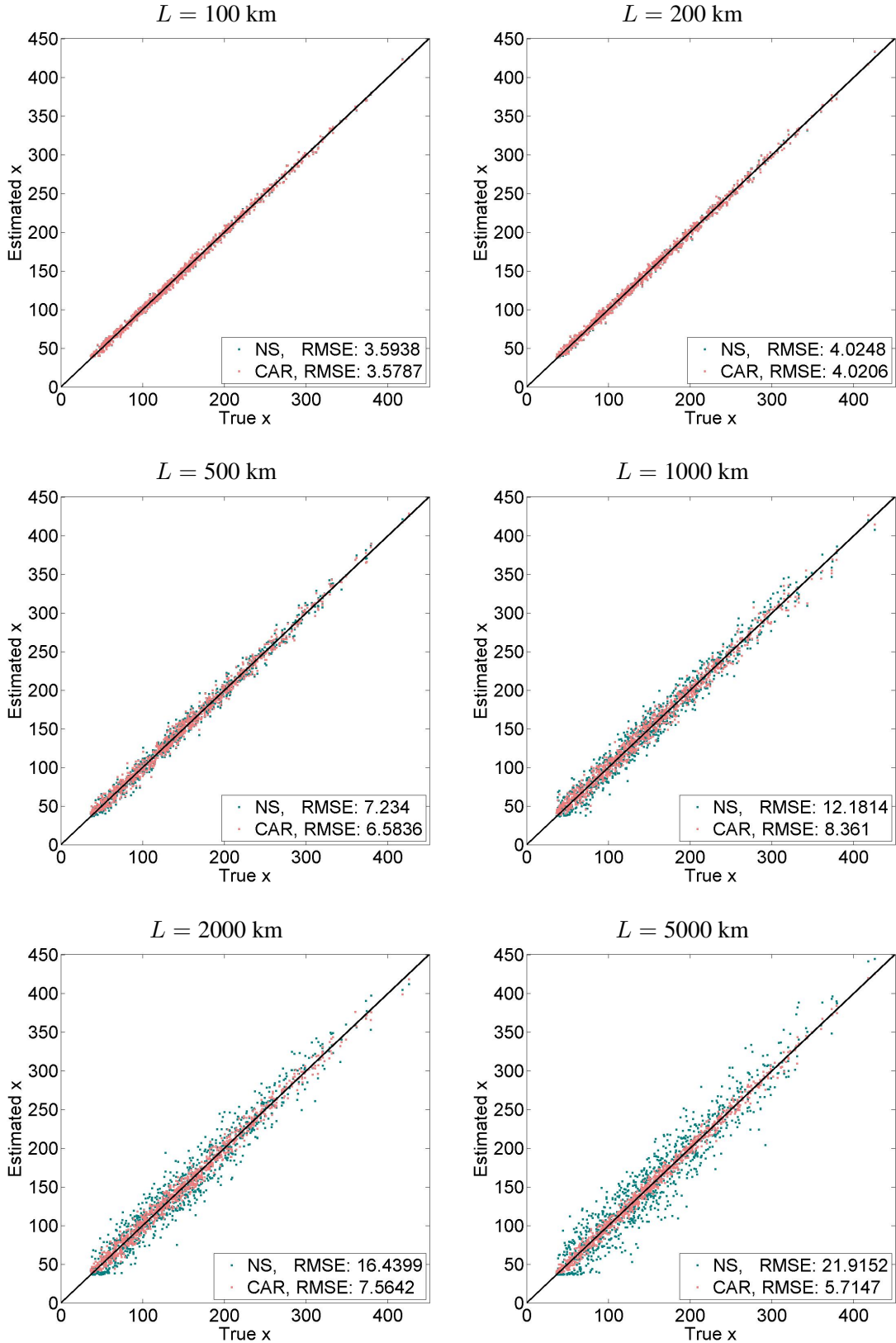


Figure 19: Scatter plots of “true” x_i versus estimated x_i (in units of Tg CO year $^{-1}$) for the source category BIOM-SAF computed from 1,000 synthetic data sets.

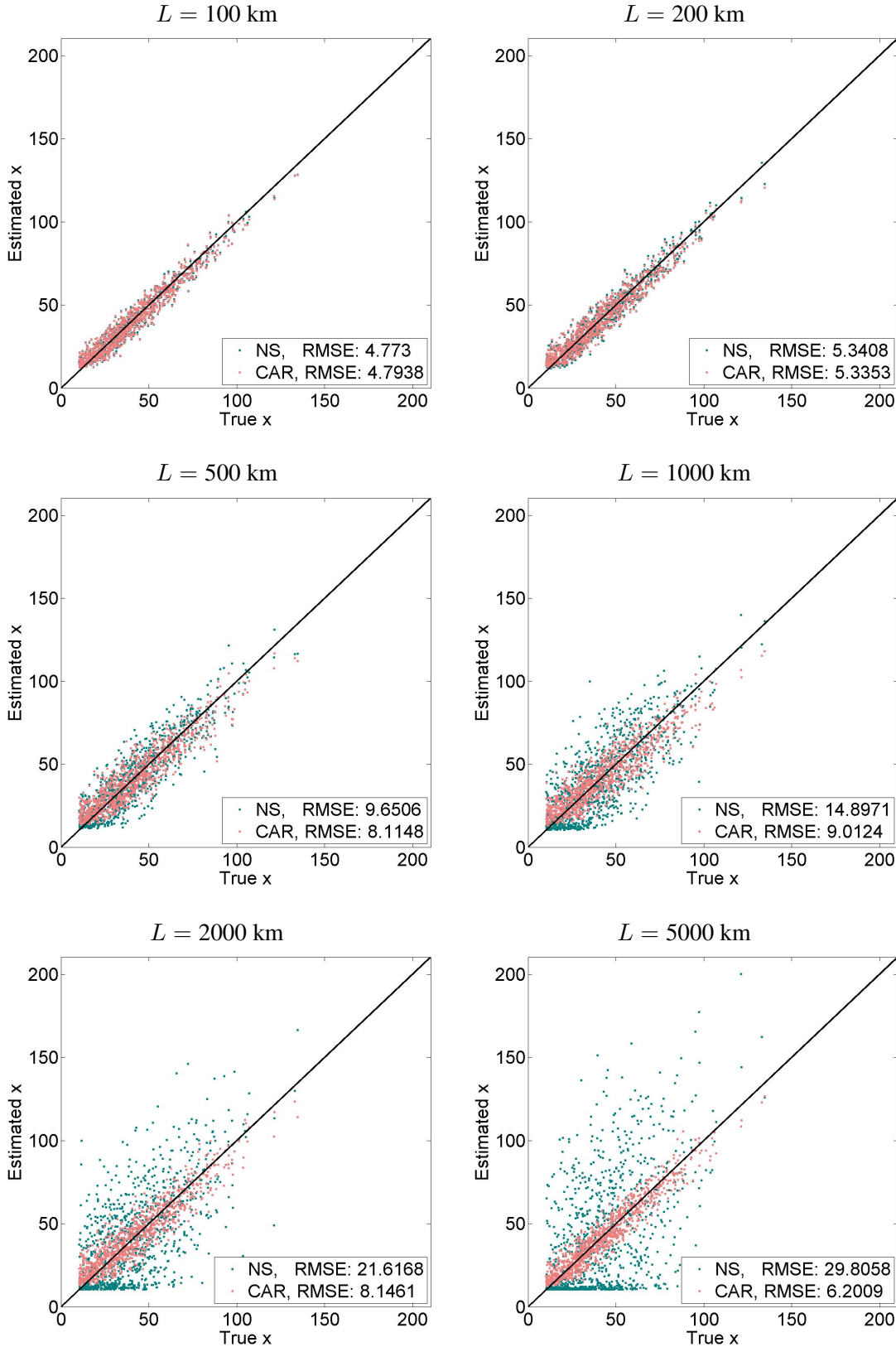


Figure 20: Scatter plots of “true” x_i versus estimated x_i (in units of Tg CO year $^{-1}$) for the source category BIOM-SSA computed from 1,000 synthetic data sets.

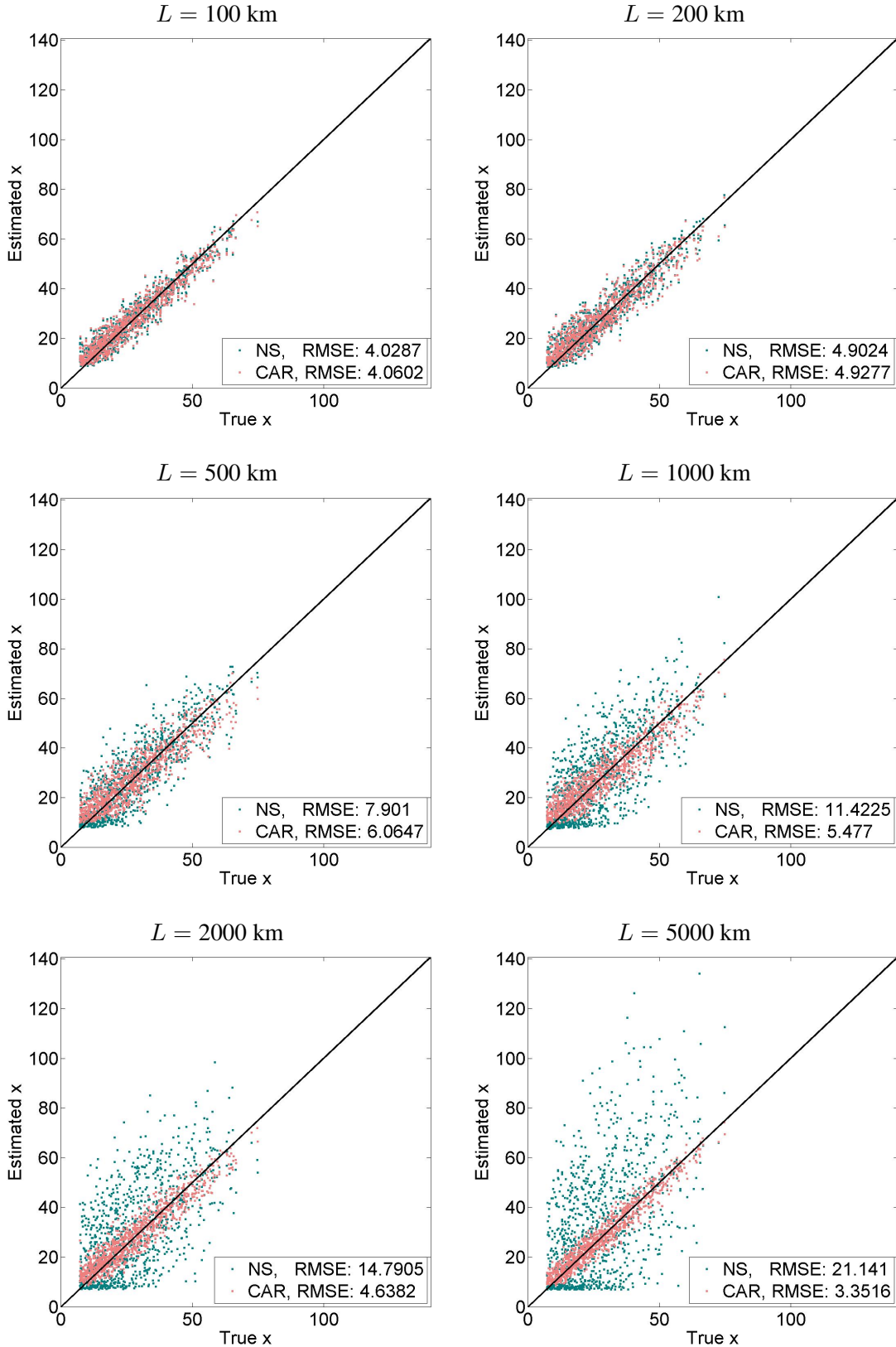


Figure 21: Scatter plots of “true” x_i versus estimated x_i (in units of Tg CO year $^{-1}$) for the source category BIOM-BOR computed from 1,000 synthetic data sets.

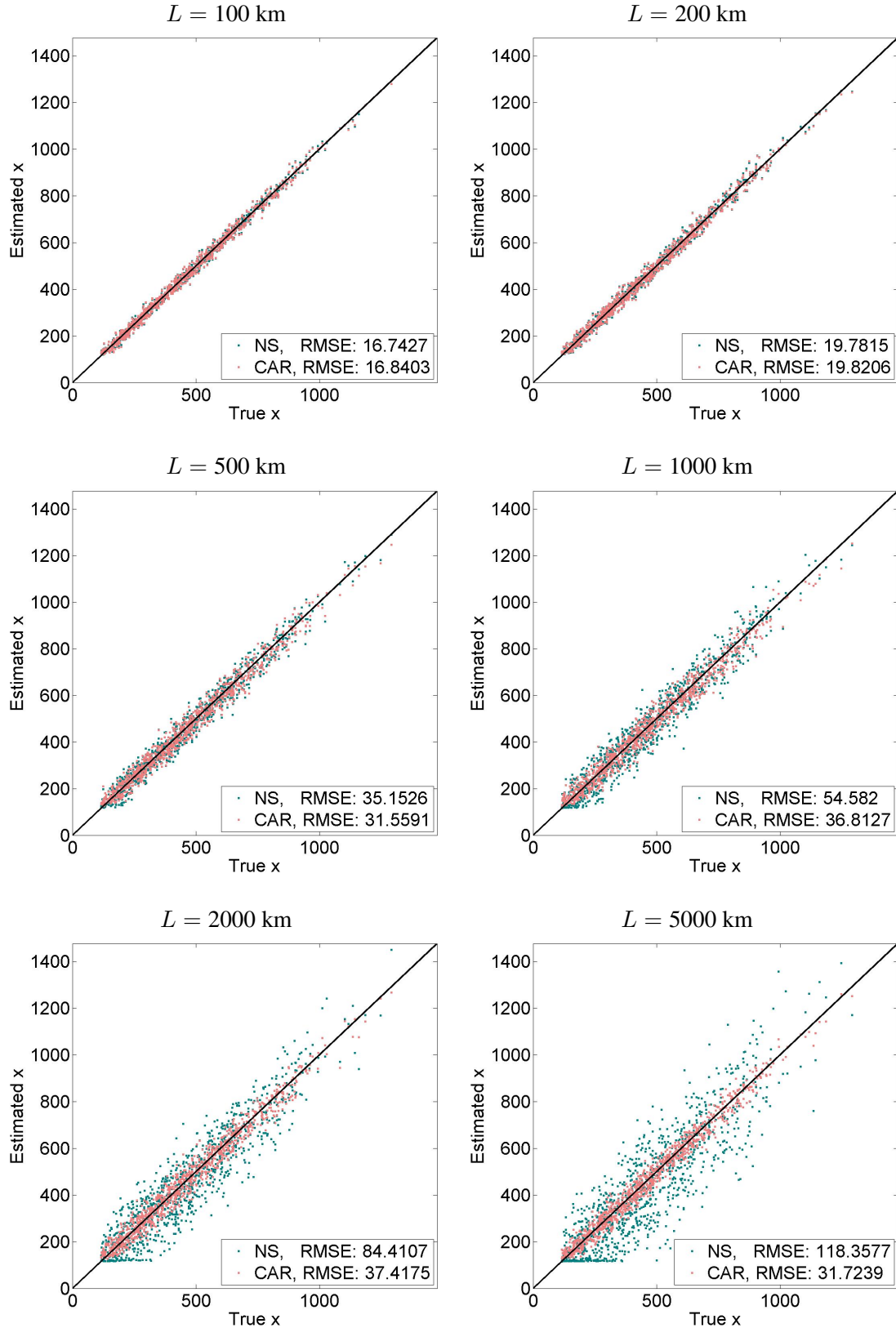


Figure 22: Scatter plots of “true” x_i versus estimated x_i (in units of Tg CO year $^{-1}$) for the source category BIOG computed from 1,000 synthetic data sets.